LBL-38240
UC-401

Center for Advanced Materials

CAM

Structural Sensitivity Studies of Ethylene Hydrogenation on Platinum and Rhodium Surfaces

M.A. Quinlan
(Ph.D. Thesis)

January 1996

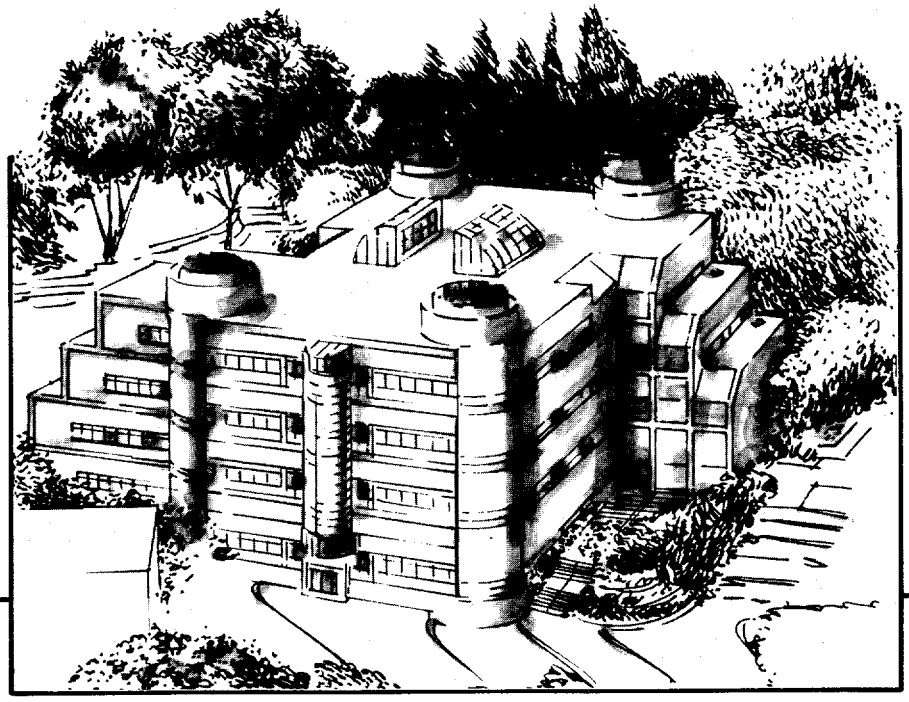

Materials and Chemical Sciences Division

Lawrence Berkeley Laboratory • University of California

ONE CYCLOTRON ROAD, BERKELEY, CA 94720 (510) 486-4755

Prepared for the U.S. Department of Energy under Contract DE-AC03-76SF00098

LBL-38240
UC-401

STRUCTURAL SENSITIVITY STUDIES OF ETHYLENE HYDROGENATION ON PLATINUM AND RHODIUM SURFACES

MICHAEL ANDREW QUINLAN

Department of CHEMISTRY
University of California

and

MATERIALS SCIENCES DIVISION
Ernest Orlando Lawrence Berkeley National Laboratory
University of California
Berkeley, California 94720

JANUARY 1996

This work was supported by the Director, Office of Energy Research, Office of Basic Energy Sciences, Materials Sciences Division, of the U.S. Department of Energy under contract No. DE-AC03-76SF00098.

Abstract

Structural Sensitivity Studies of Ethylene Hydrogenation
on Platinum and Rhodium Surfaces

by

Michael Andrew Quinlan

Doctor of Philosophy in Chemistry

University of California, Berkeley

Professor Gabor A. Somorjai, Chair

The catalytic hydrogenation of ethylene and hydrogen on the well characterized surfaces of the noble metals platinum and rhodium has been studied for the purposes of determining the relative activity of these two substrates as well as the degree of structure sensitivity. The Pt (111) and the Rh(755) single crystal surfaces, as well as Pt and Rh foils, were employed as substrates to study the effect of surface step structure on reactivity. In addition, vibrational spectroscopy studies were performed for ethylene adsorption on the stepped Rh(755) surface .

The catalytic reaction were obtained using a combined ultrahigh vacuum chamber coupled with an atmospheric pressure reaction chamber that functioned as a batch reactor. Samples could be prepared using standard surface science techniques and characterized for surface composition and geometry using Auger Electron Spectroscopy and Low Energy Electron Diffraction.

A comparison of the reactivity of Rh(111) with the results from this study on Rh(755) allows a direct determination of the effect of step structure on ethylene hydrogenation activity. Structure sensitivity is expected to exhibit orders of magnitude differences in rate as surface orientation is varied. In this case, no significant differences were found, confirming the structure insensitivity of this

reaction over this metal. The turnover frequency of the Rh(111) surface, 5×10^1 s^{-1}, is in relatively good agreement with the turnover frequency of 9×10^1 s^{-1} measured for the Rh (755) surface. Rate measurements made on the Pt(111) surface and the Pt foil are in excellent agreement, both measuring 3×10^2 s^{-1}. Likewise, it is concluded that no strong structure sensitivity for the platinum surfaces exists.

High Resolution Electron Energy Loss Spectroscopy studies of adsorbed ethylene on the Rh(755) surface compare favorably with the ethylidyne spectra obtained on the Rh(111) and Rh(100) surfaces. In general, the vibrational modes of the various functional groups associated with the adsorbed ethylidyne species do not differ greatly from the stepped or flat surfaces. One difference may be the observed shift in the C-C stretching frequency from 1120 cm^{-1} on the (111) surface to 1070 cm^{-1} on the stepped surface, indicating a weakening of the C-C bond due to increased bonding with the surface. This may arise from interaction with the step.

Table of Contents

1. Introduction

Consider the speculation concerning the origin of the stereoselectivity displayed by a chiral homogeneous catalyst. Common wisdom held that the product enantiomer results from the preferred binding of the prochiral olefin with the active site, often described in terms of a "lock and key" model. The contrary view was taken by Jack Halpern who argued that the evidence supports the opposite conclusion [1]. He reasoned that the predominant product enantiomer arises from the minor, less stable diasteriomer of the olefin-catalyst adduct which is often not present in detectable quantities. **The predominant adduct is a dead-end complex for its turnover frequency is much slower than that of the minor adduct.**

Immediate parallels can be drawn concerning ethylene hydrogenation on metal surfaces. Since its definitive identification as the most stable ethylene adsorption species, the role of the ethylidyne species in ethylene hydrogenation has been vigorously investigated. The single most conclusive piece of evidence negating the role of ethylidyne as a reactive intermediate is the radio tracing studies performed on an authenticated ethylidyne overlayer indicating that its turnover frequency is 10^3 to 10^6 times slower than the rate of ethylene hydrogenation. Still the role of ethylidyne is implicated in reported reaction schemes. Indeed, it is tempting to involve the influence of chemical species which may be present at coverages of up to 25% of a monolayer on the catalytic surface. One such mechanistic scheme uses the

ethylidyne overlayer as a provider of hydrogen atoms to the weakly adsorbed ethylene molecule [2]. Another mechanism ascribes a not so active role but uses a forest and trees type analogy to describe the active site as clearings within a regions of mobile ethylidyne species, in the words of the author a "twinkling surface", ever changing but always present in small quantities [3].

The chemical history of ethylidyne has been well characterized over single crystal metal surfaces of limited variation in geometry as a function of temperature [4]. Ethylene hydrogenation reaction studies employing single crystal surface substrates have been performed only over the basal surfaces of platinum and rhodium over a limited temperature range. The primary goal of this study is to perform careful kinetic studies using single crystal substrates over temperature ranges which span the formation and decomposition temperature of the ethylidyne species in order to elucidate any possible role in the ethylene hydrogenation reaction. Complementary studies of ethylene adsorption on basal and vicinal surfaces would allow adsorbate stability conditions to be assessed. These studies would employ the use of multiple single crystal as well as foil substrates with differing surface geometries in order to directly test the structural sensitivity of this reaction(vide infra).

A secondary goal of this work is to help resolve conflicting observations made regarding the relative activity of the noble metals platinum and rhodium. In 1984 the following comparison of the relative activity of the (111) surfaces of platinum and rhodium for ethylene hydrogenation under identical conditions of temperature and reactant partial pressures (Figure 1(A)) [5]. Rhodium is indicated to be an order of magnitude higher in activity than the platinum (turnover rates of 155 s^{-1} vs 12 s^{-1}). Surprisingly, in late 1986, the relative activity of the two metals were reported

A.

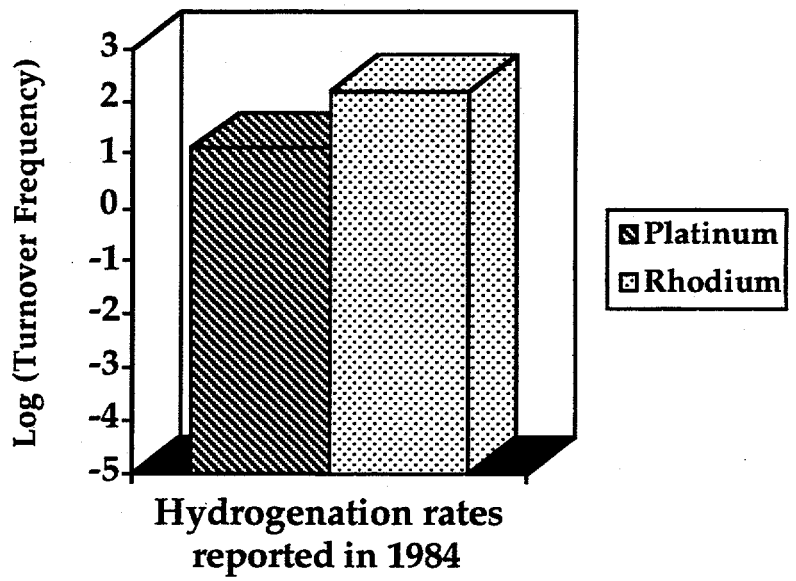

B.

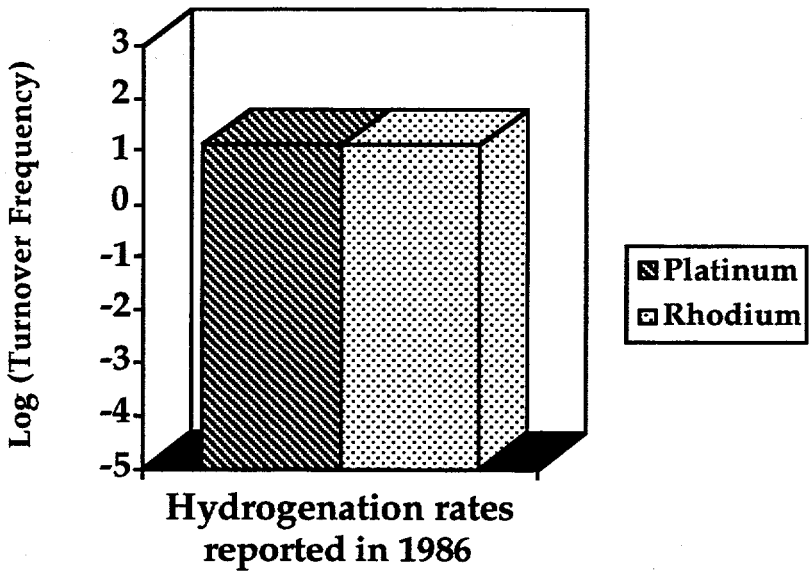

Figure 1. Ethylene hydrogenation rates over (111) surfaces of platinum and rhodium.

to be equal to that of the earlier reported absolute activity on the platinum (111) surface (Figure 1(B)) [6]. The data obtained over the platinum (111) has since been critically evaluated in light of experiments performed using supported platinum catalysts and platinum foils[7]. A comparison of the results obtained using these substrates indicated that the Pt(111) results were anomolously low. The proposed explanation for the discrepancy relies heavily on the known poisoning effect of acetylene on the ethylene hydrogenation reaction over platinum and suggests that reactant contamination is the reason that the anomolously low reaction rates were obtained.

The secondary role of this work is then defined as both clarifying the relative activity of platinum versus rhodium as well as verifying the absolute activity of platinum.

1.1. References

1. J. Halpern, Science 217(1982) 401.
2. D. Godbey, F. Zaera, R. Yeates and G. A. Somorjai, Surf. Sci. 167 (1986) 150.
3. R. Joyner, unpublished manuscript, 1992.
4. H. Ibach and D. L. MIlls, Electron Energy Loss Spectroscopy and Surface Vibrations, Academic Press, New York (1982).
5. F. Zaera, Ph.D. thesis, University of California, Berkeley, 1984.
6. B. E. Bent, Ph.D. thesis, University of California, Berkeley, 1986.
7. F. J. Rivera-Latas, R. A. Dalla Betta, M. Boudart, AIChE. J. 38 (1992) 771.

2. Ethylene Hydrogenation: Main Features and Mechanisms

2.1 An Overview of C_2 Surface Chemistry

Although the global kinetics of ethylene hydrogenation are well described by generalized mechanistic schemes, the energetics of all significant elementary steps have yet to be determined. Even the simplest of olefin hydrogenations, this ethylene conversion reaction appears not to proceed down a simple sequential reaction pair coupling pathway. The identification of dehydrogenation reactions as elementary steps to hydrogenation appears to challenge the simplistic picture of a concerted addition of hydrogen atoms across the carbon-carbon double bond as depicted in numerous undergraduate organic textbooks.

There is a consensus on several characteristics of this reaction. It is generally agreed the observed activation energy for the overall reaction is in the range of 7-10 kcal mol^{-1} over a variety of metal catalysts [1,2]. No structure sensitivity has been demonstrated either by classical methods exploring changes in reaction rate with metal particle size or by direct methods employing well characterized crystalline substrates [3,4]. Adsorption studies of ethylene on metal surfaces have clearly demonstrated that at low temperatures, ethylene is molecularly bound to the surface with the axis of

the carbon-carbon bond parallel to the surface in both pi and di sigma configurations. With increasing temperature, a series of decomposition reactions take place resulting in the formations of the stable ethylidyne species. Carbon-14 radiotracer studies [5] studies demonstrate that this ethylidyne species in not an active intermediate in ethylene hydrogenation because it has turnover frequencies orders of magnitude slower than that of ethane formation. In situ IR spectroscopy studies show that ethylene is efficiently hydrogenated in a range of temperatures and hydrogen partial pressures in which the presence of adsorbed ethylidyne is not detected. However, under most reaction conditions, generally low temperatures and high ethylene partial pressures, the hydrogenation reaction takes place in the presence of this adlayer.

The energetics of the reaction path to ethylidyne has also been well studied. The activation energy of ethylidyne formation from adsorbed ethylene has been directly measured by using such diverse techniques as LITD/FTMS, SSIMS, NMR and NEXAFS, TPD and FT-IR (Table 2.1). There is a remarkable agreement among these diverse techniques concerning the energetics of ethylidyne formation.

Adsorption studies on well characterized surfaces indicate a strong dependence of ethylidyne stability on surface geometry, four fold sites being unstable with respect to the three fold sites of FCC (111) surfaces [17]. In addition, stable surface species other than the ethylidyne such as ethylyldyne have been identified by HREELS on vicinal metal surfaces [32]. The success of semi-empirical methods in modeling the stability of the ethylidyne species as a function of binding site geometry has been demonstrated [33].

Experimental method for investigating surface reactions can be classified as direct or indirect. The most direct methods involve following the temporal changes in surface coverage under isothermal conditions by spectroscopic methods. The activation energies are then calculated from the Arrhenius plots of the rate constants for either the elementary step under investigation or the assumed rate limiting step for the reaction sequence. Methods which cannot continuously monitor product concentration or extent of conversion at the reaction temperature rely on the integrity of anneal and quench procedures. Some indirect methods follow only the disappearance of the initial reactant species and must rely on the assumption of a single reaction pathway or else account for branching reactions by other methods. Also included in Table 2.1 are indirect determinations of elementary reaction kinetics obtained from multi-parametric fitting of experimental data, such as TPD spectra. Barriers for the active chemisorption of alkyl species were estimated from the activation energies for the H-D exchange of the parent hydrocarbon.

Both direct, NMR [15], NEXAFS [20] , FT-IR [24], SSIMS [6], and indirect, TPD [7,9,14] and LITD-FTMS [27], methods are in good agreement for the overall energetics of the reaction in which adsorbed ethylene is thermally converted to the ethylidyne species. These experiments which monitor the buildup of methyl protons (NMR), surface C-C bond lengths of 1.5 angstroms (NEXAFS), or the characteristic 1339 cm^{-1} symmetric CH_3 bend(FTIR), yield activation energies of 15.2, 15.0 and a range of 13-18 kcal mol^{-1}. SSIMS measurements which follow the concentration of sputtered C_2H_3 fragments also yield an activation energy of 15 kcal mol^{-1}. Indirect methods which follow only the extent of reactant conversion also give reasonable agreement

with the more direct methods. LITD-FTMS activation energy results were 14.9 kcal mol^{-1}. Such a result gives confidence that the competing reactions of ethylene desorption and ethane formation and desorption were competently measured by the complimentary Auger studies.

Indirect methods which analyze the reaction limited hydrogen thermal desorption spectrum for the ethylene to ethylidyne transformation give values of 18.4, 17 and 18.5 kcal mol^{-1}. Thermal desorption traces of ethane resulting from the simultaneous self hydrogenation of adsorbed ethylene were also analyzed using these methods. The rate limiting step for both hydrogen desorption as well as ethane production was assumed to be the same rate limiting step for the ethylidyne formation. Activation energies for self hydrogenation were 18±4, 15±1, and 17.5 kcal mol^{-1}. All these values are in reasonable agreement with those obtained from the analysis of the low temperature hydrogen desorption peak indicating that the same rate limiting step may be being measured in all cases.

Two methods were generally used to analyze the reaction limited desorption spectra. The first, commonly referred to as the Redhead method [24] uses the temperature of the peak maximum and an assumed pre-exponential factor, usually 10^{13} s^{-1}, appropriate for a first order unimolecular decomposition reaction, to calculate the activation energy. Other methods use both the peak temperature maximum and the full width of the peak at half maximum as described by Edwards [25] or by Aris and Chan [26]. Good agreement between these methods was found by S. M. Davis for the low temperature hydrogen desorption peak indicative of ethylidyne formation [5]. Both the Redhead and the Edwards method yield 18 kcal mol^{-1}, which is also in agreement with the value of 17±3 kcal mol^{-1} obtained by Godby using the

method of Aris and Chan [7]. However, for the higher temperature reaction limited hydrogen desorption peak indicative of ethylidyne decomposition, the Redhead method give a value of 30 or 30.8 kcal mol^{-1} versus 23 kcal mol^{-1} by the method of Edwards [5].

A normal kinetic isotope effect was observed for the reaction of C_2D_4 to C_2D_3 which supports the assumption that the rate limiting barrier measured in all cases was the initial hydrogen abstraction from the ethylene [20]. In further support of this assumption, the analysis of the reaction limited ethane desorption spectrum from the surface reaction of adsorbed ethyl and adsorbed hydrogen yielded values of 12 kcal mol^{-1} and 16±2 kcal mol^{-1} [7,10]. Godbey calculates an activation barrier of 2 kcal mol^{-1} for the surface reaction of ethylene to form ethyl plus hydrogen [7]. Some disagreement is noted in studies of the dehydrogenation of ethyl groups to ethylene. Values of 7±2 and 13 kcal mol^{-1} are reported [8,11].

The activation energy for the conversion of vinylidene(CCH2) to ethylidyne was determined to be 9.3 kcal mol^{-1} using proton NMR [28]. An unusually low pre-exponential of 3.8 X $10^{3\pm2}$ s-1 resulted from this calculation. H-D exchange parameters were not explicitly calculated but were assumed to be in the range of 11.8 to 16.8 kcal mol^{-1} with corresponding pre-exponentials of 4 X $10^{7\pm2}$ s^{-1}. The activation energy for the H-D exchange of ethylidyne had previously been determined to be 14.3±0.3 kcal mol^{-1} with a pre-exponential of 4 X10^2 s^{-1} [11]. An apparent resolution of these two diverse values resulted from the recalculation of the SSIMS data by the NMR group taking into account the surface hydrogen coverage by using the method of Ertl [12]. A corrected activation energy of 11.8 kcal mol^{-1} was then obtained. The

activation energy for the formation of ethyl from ethane was estimated from the activation energy for H-D exchange in ethane to be 19±7 kcal mol^{-1} [13].

A summary of many of the important reactions of ethylene and ethylene-derived species is contained in Table 2.2

Table 2.1. Experimental activation energies for surface reactions of C_2 species on Pt surfaces

Hydrogenation reactions

Reaction	Energy (kcal•mol^{-1})	Technique	Ref.
$CH_2CH_3 + H = C_2H_6$	12	TDS (C_2H_6)	10
	16±2	SSIMS	11
	16±1	TDS (C_2H_6)	7
$CH_2CH_2 + H = C_2H_5$	2	fit to TDS	7
	15±1	TDS (C_2H_6)	8
	13	estimate	8
$CCD_2 + H = CCD_2H$	9.3±2.5	NMR	28

Table 2.1 (continued). Experimental activation energies for surface reactions of C_2 species on Pt surfaces

Dehydrogenation reactions

Reaction	Energy (kcal•mol^{-1})	Technique	Ref.
$CH_2CH_2 = CCH_3 + H$	15.2±2	NMR	15
	15.0±1	NEXAFS	20
	16±3	FTIR	24
	15	SSIMS	6
	14.9±1.4	LITD-FTMS	27
	18.4±1.7	TDS(H_2)	14
	17±3	TDS(H_2)	7
	18.5	TDS(H_2)	9
	18±4	TDS(C_2H_6)	7
	17.5	TDS(C_2H_6)	9
$C_2H_5 = C_2H_4 + H$	7±2	TDS(C_2H_4)	8
	13	SSIMS	11
$CD_3CH_2 = CD_2CH_2 + H$	6±0.5	TDS(CD_2CH_2)	21
$CCD_3 = CCD_2 + D$	14.3±0.3	NMR	15
	7.2±0.3	SSIMS	11
	11.8	SSIMS*	15
$C_2H_6 = C_2H_5 + H$	19±7	H-D exchange	13

* recalculation of data presented in reference [11] by authors of reference [15].

2.1.1 References

1. G. C. Bond, Catalysis by Metals, Academic Press, London, 1962.

2. D. D. Eley, The Catalytic Hydrogenation of Ethylene, in "Catalysis Vol. III, P. H. Emmett ed., Reinhold Publishing Corporation, New York, 1955.

3. M. Boudart, Adv. Catal. , 20 (1969) 153.

4. M. Boudart and G. Djega-Mariadassou, Kinetics of Heterogeneous Catalytic Reactions, Princeton University Press, Princeton, New Jersey, 1984.

5. S. M. Davis, F. Zaera, B. E. Gordon and G. A. Somorjai, J. Catal. 92 (1985) 240.

6. K. M. Ogle, J. R. Creighton, S. Akhter and J. M. White, Surface Sci. 169 (1986) 246.

7. D. Godbey, F. Zeara, R. Yeates and G. A. Somorjai Surface Sci. 167 (1986) 150.

8. F. Zaera, J. Phys. Chem. 94 (1990) 5090.

9. R. G. Windham, M. E. Bartram and B. E. Koel, J. Phys. Chem. 92 (1988) 2862.

10. F. Zaera, Surface Sci. 219 (1989) 453.

11. K. G. Lloyd, B. Roop, A. Campion, and J. M. White, Surf. Sci. 214 (1989) 227.

12. K. Christman, G. Ertl, T. Pignet, Surf. Sci. 54 (1976) 365.

13. F. Zaera and G. A. Somorjai, J. Phys. Chem. 89 (1985) 3211.

14. M. Salmeron and G. A. Somorjai, J. Phys. Chem. 86 (1982) 341.

15. D. B. Zax, C. A. Klug, C. P. Slichter and J. H. Sinfelt, J. Phys. Chem. 93 (1989) 5009.

16. Dumesic, J. Phys. Chem. 96 (1992) 1880.

17. Backman and Maesel, J. Vac. Sci. Tech. A9(1991)1789.

18. D, B, Zax, Chem. Phys. Lett. 151 (1988) 227.

19. F. Zaera J. Am. Chem Soc. 111(1989)4240.

20. F. Zaera, D. A. Fischer, R. G. Carr, E. B. Kollin and J.L. Gland in Molecular Phenomena at Electrode Surfaces; ACS Symposium Series No. 378; M.P. Soriaga, Ed.,ACS, Washington, D. C. 1988.

21. F. Zaera , J. Phys. Chem. 94 (1990) 8350.

22. G. Comsa, Surf. Sci. 111 (1981) 519.

23. N. Avery, Langmuir 4 (1988) 445.

24. S. B. Mohsin, M. Trenary, H. J. Robota, Chem. Phys. Lett. 154 (1989) 511.

25. J. R. Creighton, K. M. Ogle and J. M. White, Surf. Sci. 138 (1984) L137.

26. T. P. Beebe, Jr. and J. T. Yates, Jr., J. Am. Chem. Soc. 108 (1986) 663.

27. C. L. Pettiette-Hall, D. P. Land, R. T. McIver Jr., and J. C. Hemminger, J. Phys. Chem. 94 (1990) 1948.

28. C. A. Klug, C. P. Slichter and J.H. Sinfelt, J. Phys. Chem. 95 (1991) 2119.

29. P. A. Redhead, Vacuum 12 (1962) 203.

30. D. Edwards, Jr., Surf. Sci. 54 (1976) 1.

31. C. M. Chan and R. Aris and W. H. Weinberg, Appl. Surf. Sci. 1(1978)360.

32. E. Yagasaki, A. L. Backman, and R. I. Masel, J. Phys. Chem. 94 (1990) 1066.

33. P. D. Ditlevsen, M. A. Van Hove and G. A. Somorjai, Surf. Sci. 292 (1993) 267.

2.2. Structure Sensitivity

Strictly speaking, the rate of reaction on a catalytically active surface, the turnover frequency, is the number of times that the overall reaction takes place per catalytically active site and per unit time [1]. While the concept of an active site is easy to imagine, the direct measurement of the number of such sites defies present ability. Very often a compromise is made in which one measures the number of exposed surface atoms and then relates the rate to this areal measurements. This compromise is predicated on the assumption that the active site is either a single surface atom or a fixed number of contiguous surface atoms (the so called catalytic ensemble). This is a relatively easy measurement for metals using dihydrogen, carbon monoxide or dihydrogen-oxygen titration. What of more complex catalysts such as the many component iron based ammonia synthesis catalyst? One of the great advances in the field of catalysis occurred as a result of the selective chemisorption studies of Paul Emmett, wherein he showed that the total surface area of the catalyst could be distinguished from the metallic and the oxide components of the catalyst by their differing chemisorption ability [1].

When reaction rates using supported metal catalysts are measured as the mean particle size of the metal is varied, reactions seem to fall into two types. For certain classes of reactions, Table 2.2 [1,2], the turnover frequency for a particular reaction is invariant as the size of the metal crystallite is varied in size especially in the range of 10 to 100 A. For others, the reaction rate changes by orders of magnitude through this range. Reactions

demonstrating this particle size effect are usually called structure sensitive reactions [2,4]. This effect can result in both decreased or increased reactivity.

The relationship between metal particle size and surface structure can be seen by considering simple geometric models of small metal crystallites. Van Hardeveld and Hartog have made detailed calculations of the shapes and statistics of surface atoms and sites for many type of ideal metal crystallites [7]. The fraction of surface atoms having coordination numbers from say 4 to 9 can be calculated for uniform cubo-octahedron particles of fcc metals. These fractions change most rapidly in the range of particles sizes from 10 to 50 A. If a reactive site were to be associated with a particular type of coordination, great changes in reactivity would be predicted. It needs to be mentioned that the titration method must be insensitive to coordination. For the case of the ammonia synthesis catalyst, attempting to count the number of surface iron atoms by high temperature dinitrogen chemisorption yields the erroneous conclusion of structure insensitivity, because in this case, the number of reactive centers varies directly as the number of nitrogen chemisorption sites.

The fundamental nature of the metal particle may also change as dimensions approach that of metal clusters. A number of theoretical and experimental studies have indicated that the electronic properties of metal clusters are considerably different than the bulk metal [8]. Here structural sensitivity must be considered in the same vein as reaction studies using different catalytically active metals.

Reaction studies on clean metal surfaces of varying crystallographic orientations provide a direct method of testing a reaction for structural sensitivity. The classical method required multiple supported catalyst

Table 2.2. Some examples of reactions classified by structure sensitivity [1,2].

Structure Insensitive	Structure Sensitive
Hydrogenation of olefins	Hydrogenolysis of alkanes
Dehydrogenation of cyclohexane	Dehydrocyclization of n-heptane
Isomerization of large alkanes (>C_5)	Isomerization of light alkanes (<C_5)
Hydrogenation of cyclopropane	Ammonia synthesis
Carbon monoxide oxidation	

samples of different dispersions, with crystallite dimensions in the range of 10 to 100 angstroms [9]. The larger metal crystallites were assumed to consist largely of the low index basal planes, mostly the (111) orientation. Appropriately, (111) or (100) surfaces are commonly used as the reference surface. As the crystallite size decreases below the critical size of 50 angstroms, more irregular surfaces are formed which are indirectly modeled by the use of high Miller indices surfaces. There are no rules for which high Miller indices surfaces are appropriate to use to mimic these small crystallite catalysts. An early example of substrate selection is a 1984 study of n-hexane conversion reactions which demonstrated structurally sensitivity for n-hexane aromatization to benzene using four different platinum single crystal surfaces (10,8,7), (111), (100), and (13,1,1) [6].

Extreme differences in ammonia synthesis activity were noted using iron (110), (210), (100) and (221) surfaces [10] and rhenium (1121), (1120), (1010) and (0001) surfaces [11]. While the order of activity roughly parallels surface roughness, it also serves to expose certain highly coordinated metal atoms present in the second and third layers which are though to be the sites of high catalytic activity.

One can choose a particular surface feature such as a step edge and prepare a series of single crystal surface substrates over which the step density is varied by an order of magnitude. The range over which the density of surface features can be varied, step frequency for example, is limited by the practical considerations of the preparation of "perfect" defect free surfaces. One can ignore the subtleties of coordination site distribution and use surface roughness, defined as the reciprocal of the packing density [5], as the measure of deviation from the atomically flat basal surface. Both stepped and kinked

surfaces have been used. For this study, stepped surfaces of 755 orientation consisting of six atom wide terraces of (111) orientation having monoatomic height steps of (111) orientation were used and compared to the flat (111) surface. It was hoped that this particular geometric site offered the reaction a sufficiently high density of particularly active sites (the steps) that any structural sensitivity would be evident.

2.2.1. References

1. M. Boudart and G. Djega-Mariadassou, Kinetics of Heterogeneous Catalytic Reactions, Princeton University Press, Princeton, New Jersey, 1984.
2. G. A. Somorjai and J. Carrazza, Ind. Eng. Chem. Fundam. 25 (1986)63.
3. G. C. Bond, Acc. Chem. Res. 26 (1993) 490.
4. G. C. Bond,R. H. Cunningham, and J. C. Slaa, Topics in Catalysis 1 (1994)19.
5. F. Jona and P. M. Markus, in : The Structure of Surfaces (Springer Verlag, Berlin, 1988) p. 80.
6. S. M. Davis, F. Zaera and G. A. Somorjai, J. Catal. 85 (1984) 206.
7. R. van Hardeveld and F. Hartog, Surface Sci. 15 (1969) 189.
8. L. M. Falicov and G. A. Somorjai, Proc. Natl. Acad. Sci. USA, 82 (1985) 2207.
9. C. N. Satterfield, Heterogeneous Catalysis in Industrial Practice, 2nd ed, McGraw Hill, New York, 1991.
10. N. D. Spencer, R. C. Schoonmaker and G. A. Somorjai, J. Catal. 74 (1984) 129.
11. N. D. Spencer and G. A. Somorjai, J. Catal. 78 (1982) 1112.

2.3. The Kinetics of Ethylene Hydrogenation

2.3.1. Mechanisms and Rate Expressions

One of the earliest proposed mechanisms for ethylene hydrogenation came from Rideal, who proposed that gaseous hydrogen directly reacts through impact with a chemisorbed ethylene layer by the reaction mechanism which bears his name today [1].

$$H_2(g) + C_2H_4(ads) \rightarrow C_2H_6(g)$$

Thomson and Webb attempted to consolidate the following observations regarding the kinetics of ethylene hydrogenation [2] :

1. Simplified kinetics applied to different mechanisms lead to identical rate expressions.
2. The activation energy for hydrogenation varies little with the nature of the metal surface.
3. The reaction appears structure insensitive.
4. The reaction takes place in the presence of a strongly adsorbed hydrocarbon layer.

They concluded that the reaction takes place by hydrogen transfer between an adsorbed hydrocarbon species and the adsorbed olefin.

During the 80's, reaction mechanisms appeared which identified the adsorbed hydrocarbon proposed by Thomson and Webb as the ethylidyne species [3,4].

Many of the features of ethylene hydrogenation can be accounted for by the classical olefin hydrogenation mechanism of Horiuti and Polanyi [5]. The proposed sequence of elementary steps follows:

$$H_2 + 2* = 2H*$$

$$C_2H_4 + 2* = **$$

$$*C_2H_4* + H* = C_2H_5* + 2*$$

$$C_2H_5* + H* \rightarrow C_2H_6 + 2*$$

where * indicates a vacant adsorption site.

This mechanism predicts at low temperatures and pressures, a rate which is proportional only to the hydrogen partial pressure and at high temperatures and pressure a rate proportional to the square root of the hydrogen partial pressure.

The mechanism of Horiuti and Polanyi is the starting point for many other mechanisms which attempt to include different descriptions of the variety and competitive nature of the adsorption sites [6-9].

Generalized Langmuir type kinetics can be used to describe the possible reaction mechanisms for ethylene hydrogenation. Three possible model can be discussed which differ in their treatment of the adsorption sites, which can be non-competitive, competitive or a combination of the two.

I. Hydrogen and ethylene are reversibly adsorbed on a uniform surface.

$$\text{rate} = k\frac{\sqrt{b_{H_2}p_{H_2}}\, b_{C_2H_4}p_{C_2H_4}}{(1+\sqrt{b_{H_2}p_{H_2}}+b_{C_2H_4}p_{C_2H_4})^2}$$

where $p(H_2)$,$p(C_2H_4)$ are the partial pressures of hydrogen and ethylene respectively and $b(H_2)$ and $b(C_2H_4)$ are the corresponding adsorption coefficients and k is the overall rate constant.

For surfaces largely covered by ethylene,

$$1 + [b(H_2)p(H_2)]^{1/2} << b(C_2H_4)p(C_2H_4)$$

$$\text{rate} = k\frac{\sqrt{b_{H_2}p_{H_2}}}{b_{C_2H_4}p_{C_2H_4}} = k'\frac{\sqrt{p_{H_2}}}{p_{C_2H_4}}$$

II. Hydrogen and ethylene are adsorbed on two separate sites with the reaction occurring only at the interface.

$$\text{rate} = k\frac{\sqrt{b_{H_2}p_{H_2}}}{(1+\sqrt{b_{H_2}p_{H_2}})}\frac{b_{C_2H_4}p_{C_2H_4}}{(1+b_{C_2H_4}p_{C_2H_4})}$$

Again, for surfaces largely covered by ethylene such that

$$[b(H_2)p(H_2)]^{1/2} << 1 << b(C_2H_4)p(C_2H_4),$$

$$\text{rate} = kb_{H_2}p_{H_2} = k'p_{H_2}$$

III. Two types of adsorption sites exist, hydrogen is non-competitively adsorbed on the first type of sites while hydrogen and ethylene compete for the second type of sites.

$$\text{rate} = k\frac{\sqrt{b_{H_2}p_{H_2}}\,b_{C_2H_4}p_{C_2H_4}}{1+\sqrt{b'_{H_2}p_{H_2}}+b_{C_2H_4}p_{C_2H_4}}$$

where $b'(H_2)$ refers to the hydrogen adsorption constant for the second type of sites.

2.3.2. Origin of the Zero Order Dependence on Ethylene Concentration

The observation of a zero order dependence on the ethylene concentration implies that the catalytic surface is largely covered by hydrocarbon intermediates. However when published results are examined in detail, disparate conclusions regarding the dependence of the reaction rate on the initial ethylene partial pressure are seen. The gross features of this discussion apply equally well to both the platinum and rhodium substrates employed. Because of the paucity of investigations employing rhodium catalysts, most of the data presented comes from the literature of platinum catalysts.

The most striking feature of the results is the lack of agreement among researchers concerning the reaction order with respect to the ethylene partial pressure compared to the reaction order in hydrogen partial pressure or activation energy. Whereas the accumulated results in the latter appear to be normally distributed about an average near first order, the reaction order in ethylene is confidently reported as either zero or -0.5 to -0.8, in an apparent bimodal distribution. Even more puzzling is the apparent contradiction within a report when one considers the data in detail.

One author illustrates a typical product accumulation plot for the ethylene hydrogenation reaction in which over the course of 60 minutes, some 2.4×10^4 turnovers have occurred, resulting in the consumption of 80% of the initial aliquot of ethylene (Figure 2.1) [4]. The accumulated product versus time plot shows excellent linearity with no deviation from time zero to the last data point at 80% conversion. The rate of reaction is easily calculated from the slope of such plots. In a different series of experiments, the initial partial pressures of deuterium or hydrogen are

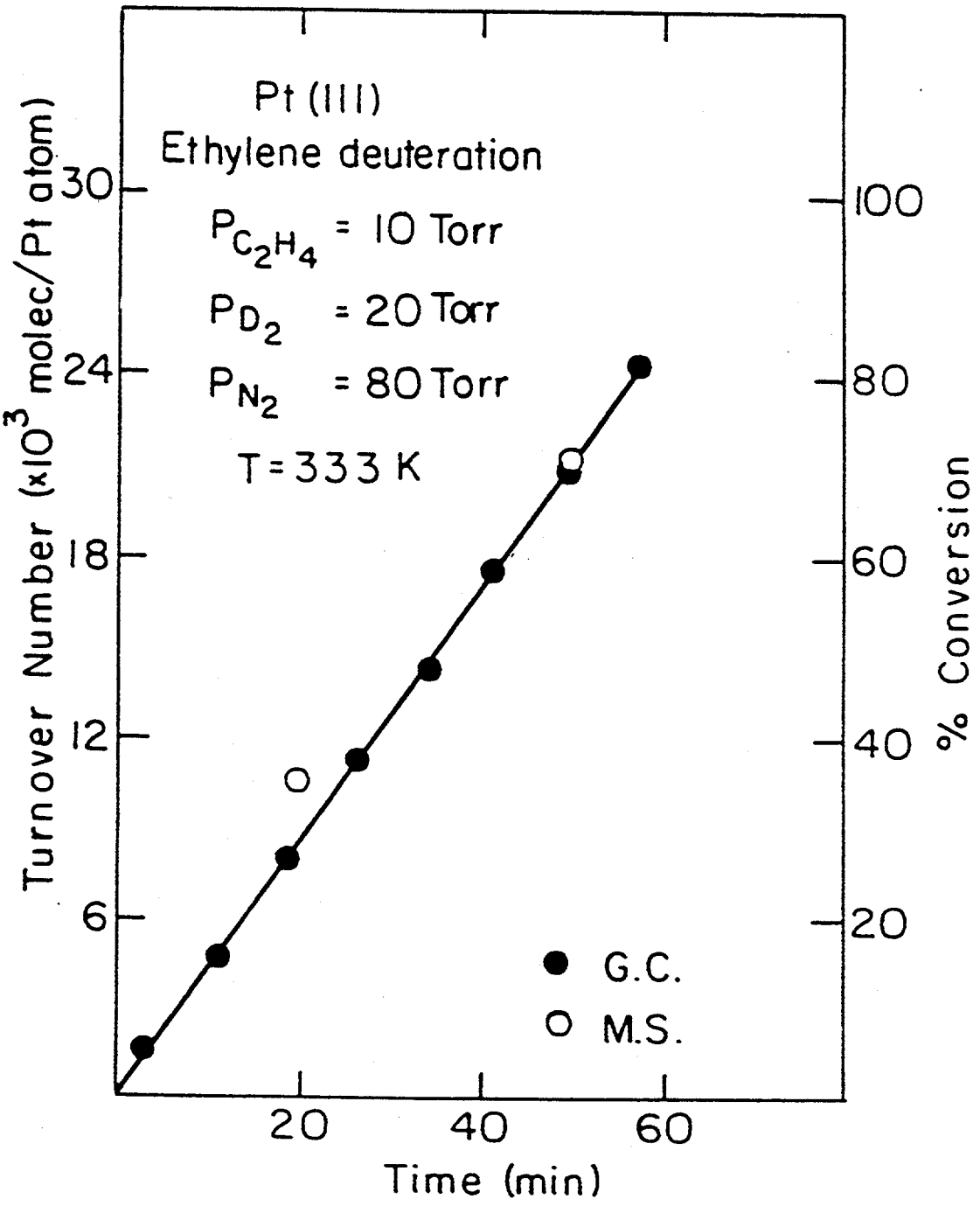

Figure 2.1. Product accumulation plot for ethylene hydrogenation on Pt(111) demonstrating zero order rate dependence on reactant partial pressures [8].

systematically varied for a series of reactions at constant temperature, from which the reaction orders in ethylene and hydrogen were calculated to be -0.6 and 1.3, respectively.

However, when one attempts to reconcile these two pieces of information by comparing the expected product accumulation plot for the condition under which those reactant reaction orders where obtained, it can be shown that strong deviation from the reported linear product accumulation should have been observed. The amount of predicted accumulated product at the end of 60 minutes reaction time far exceeds the reported concentration by amounts greater than the indicated error limits of the analysis. The calculated acceleration in rate with increasing ethylene consumption results from the reaction being run under conditions of excess hydrogen such that the overall rate is more dependent on the depletion in ethylene than the change in hydrogen partial pressure. It would require a reaction mechanism that was exquisitely dependent on the ethylene partial pressure to explain the apparent -0.6 order dependence in the range of 10 to 20 torr with a shift to zero order behavior for the range of 2 to 10 torr.

One such complex mechanism is hypothesized by the Dumesic group [10-11] in their microkinetic treatment of the ethylene hydrogenation reaction. They calculate from their proposed mechanism an overall order in ethylene which smoothly varies from -0.09 at 223 K to -0.65 at 333 K in the pressure range of 5 to 75 torr. By way of comparison, experimental values of -0.17 to -0.43 were obtained for the same range of temperature and ethylene partial pressure. As to the dependence of the reaction order in ethylene at constant temperature, only the general conclusion that the order approaches zero order at partial pressures above 75 torr and is negative at "low" ethylene

partial pressures (below 25 torr). At 5 torr, the normalized rate was approximately a factor of two greater than the rate at 25 torr. The work previously cited spans the temperature range from 300 to 370 K . According to the Dumesic mechanism, the negative reaction order behavior is be expected based on both the temperature and partial pressure range explored. No explanation, however, can offered for the observed zero order dependence of the rate during a reaction in which the ethylene partial pressure changes from 10 to 2 torr, a five fold decrease.

The kinetic order in hydrogen was investigated in detail by the Dumesic group and was also found to be temperature dependent. At a constant ethylene partial pressure of 25 torr, they reported a smooth change in the reaction order with respect to hydrogen from first order at 336 K to half order at and below 248 K. No effect of ethylene pressure was observed. Again given the temperature of 333 K in the reaction example it is surprising that no deviations from pseudo zero order kinetics were observed. This observation will be repeated during the presentation of the kinetic results of this work.

2.3.3. References

1. E. K. Rideal, International Congress on Catalysis, 1956.
2. S. J. Thomson and G. Webb, JCS Chem. Comm. (1976) 256.
3. B. E. Bent, Ph.D. thesis, University of California, Berkeley, 1986.
4. F. Zaera, Ph.D. thesis, University of California, Berkeley, 1984.
5. Horiuti and Polanyi, Trans. Faraday Soc. 30 (1934) 1164
6. G.-M. Schwab,Catalysis,d. Van Nostrand Company, New York, 1937.

7. S. Berkman, J. C. Morrell and G. Egloff, Catalysis - Inorganic and Organic, Reinhold Publishing Corporation, New York, 1940.

8. M. Boudart and G. Djega-Mariadassou, Kinetics of Heterogeneous Catalytic Reactions, Princeton University Press, Princeton, New Jersey,1984.

9. D. D. Eley, The Catalytic Hydrogenation of Ethylene, in "Catalysis Vol III, P. H. Emmett ed., Reinhold Publishing Corporation, New York, 1955.

10. R. D. Cortright et al, J. Catal. 127(1991)342.

11. J. A. Dumesic et al, The Microkinetics of Heterogeneous Catalysis, American Chemical Society, Washington D. C., 1993.

3. Experimental Techniques

3.1. Low Energy Electron Diffraction

It is not sufficient to solely rely on the information provided by Laue X-ray diffraction measurements performed during the initial phases of sample preparation to characterize the structure of the first, or first and second surface layers of the catalytic substrate. Since only those atoms belonging to these outermost layers are thought to be responsible for the observed chemistry, only techniques which are sensitive to their geometry, degree of order and the presence of ordered overlayers will provide the information necessary to correlate changes in chemistry with changes in structure.

Low energy electron diffraction can provide this information about the geometry and the degree of order of the substrate with the required surface sensitivity. In this technique, a well focused beam of monoenergetic electrons, with an energy in the range of 10 to 500 eV, impinges on the surface, typically at the normal angle of incidence. This corresponds to a de Broglie wavelength of 4 to 0.6 A which spans the range of most interatomic distances. The incident beam is scattered from the surface region of the substrate and in the presence of sufficiently large domains of two dimensional order , the scattered waves will undergo constructive interference at those certain angles which fulfill the Bragg condition. The

scattered electrons are spatially analyzed using the conventional four grid retarding field optics shown in figure 3.1. The first and fourth grids are grounded, while the second and third grids are at near the primary beam energy so as to repel the inelastic electrons. The elastically scattered electrons which remain are then accelerated onto a phosphor coated hemispherical screen. The resultant electron diffraction pattern is observed as a pattern of well defined bright spots displayed on the phosphorescent screen. The symmetry of the observed pattern reflects the symmetry of the ordered surface unit cell and the sharpness and intensity of the spots are related to the degree of surface ordering.

The surface sensitivity of the LEED technique is a consequence of the nature of the scattering ability of these low energy electrons as opposed to the X-rays used in the Laue technique. While X-rays may penetrate thousands of angstroms in the solid, these more strongly interacting low energy electrons have mean free paths of 5 to 10 angstroms. This desirable surface sensitivity is not without its drawbacks. Due to the highly interacting nature of the electron with the substrate atoms, multiple interactions become likely (unlike the case with X-ray scattering) and preclude the use of simple single scattering or kinematic theory to extract structure from the experimental data.

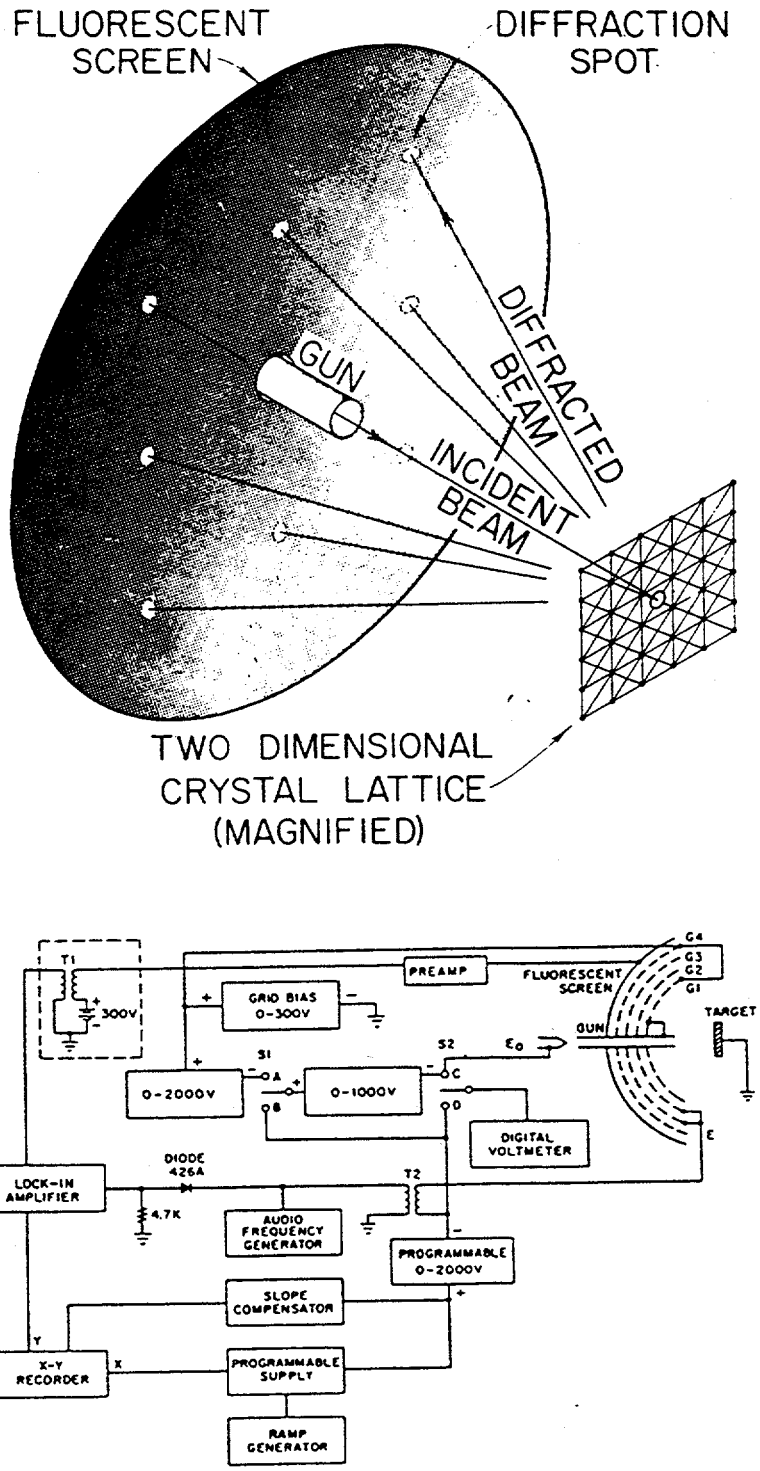

Figure 3.1. The LEED experiment and associated equipment.

The simplest demonstration of the Bragg condition can be illustrated by stepping backward one dimension.

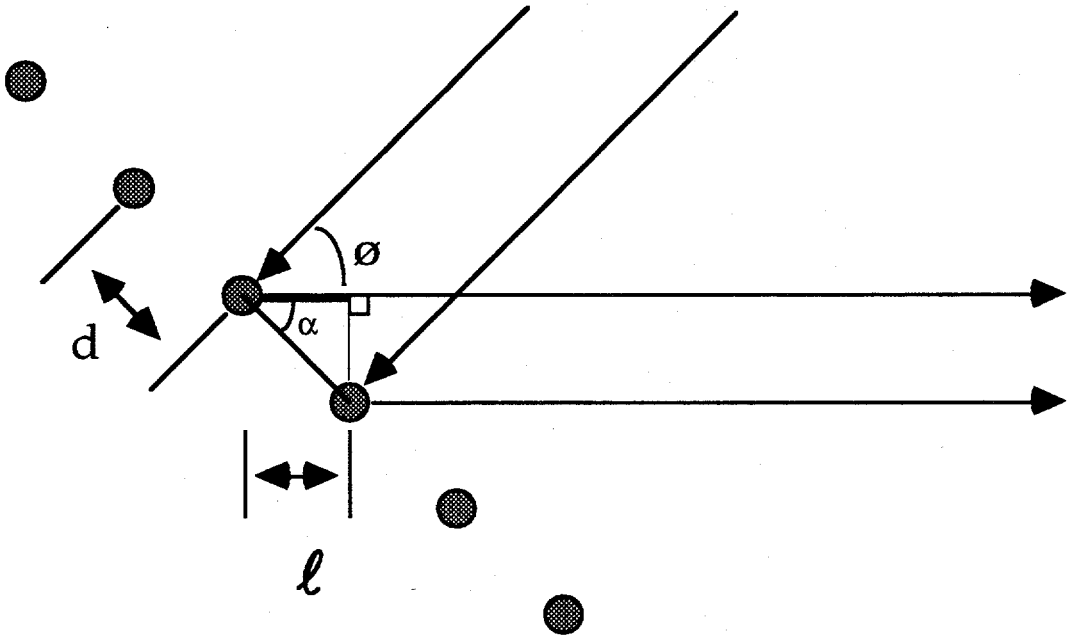

For an incoming wave impinging at normal incidence onto a one dimensional string of scattering centers, the difference in path lengths, ℓ, at a fixed scattering angle, Ø, is equal to

$$\ell = d \sin(Ø)$$

and the condition for constructive interference between out going scattered waves is given by

$$n\lambda = d \sin(Ø).$$

Extending our periodic array to two dimensions and noting that the De Broglie wavelength of an electron, λ, is

$$\lambda = (150/eV)^{1/2}$$

yields

$$\sin(\emptyset) = n/d_{hk}\,(150/E(eV)^{1/2}$$

as our statement of the Bragg condition for our electron wave scattering from our two dimensional solid with periodicity d_{hk}.

LEED studies can be performed in both a qualitative and quantitative manner. This division is reminiscent of the elements of surface crystallography. Remember that the two elements of the two dimensional surface geometry are the lattice and the basis. The unit cell is the collection of lattice points which has the property of translational symmetry. The basis is the collection of atoms associated with each lattice point. Qualitative LEED makes use solely of the symmetry of the electron diffraction pattern at any one incident energy to learn information regarding the unit cell of the surface layer.. For instance, the pattern of spots caused by diffraction from the clean surface may allow one to make judgments regarding the clean surface unit lattice if gross reconstructions cause the symmetry of the uppermost layer to deviate from what would be expected from simple bulk termination. Two well known examples of this are the complex LEED patterns from the clean Pt(100) and Au(100) which appear instead of the simple square patterns predicted from bulk termination. Additional spots which result from the

adsorption of adsorbates can be similarly analyzed to gain information about the size and orientation of the new surface unit cell with respect to the geometry of the substrate. In all these studies one learns only the geometry of the unit cell with respect to the substrate unit cell. No information regarding the number of atoms or molecules in the unit cell, or the details of bond lengths and bond angles can be obtained. A most relevant example is the controversial coverage determination of the (2X2) phase of ethylidyne on Pt(111). Support exists for both the interpretation of the pattern as a p(2X2) pattern with O = 0.25[7-9] as well as experiments which support a coverage determination of 0.50[10-12] corresponding to the superimposition of three degenerate (2X1) patterns rotated 120 degrees with respect to each other.

Further analysis is necessary to obtain information regarding the element of the basis. All information concerning the local geometry of the adsorbate-substrate bond or the structure of the adsorbate is contained within the relationship of the intensity of the diffraction spot with the incident electron beam voltage. By comparing the experimental intensity versus voltage curves (I (V) curves) with theoretical diffraction models which take into account multiple scattering , the various bond lengths and angles can be estimated. Advances in computational methods have been developed so as to allow automated search methods to be performed[6]. In this way, a large number of likely models of surface structure may be compared to the experimental data in a timely manner, giving greater confidence in the conclusions reached.

3.1.1. References

1. G. A. Somorjai, Chemistry in two dimensions; Cornell University Press: Ithaca, NY, 1981.

2. M.A Van Hove, S. Y. Tong, Surface Crystallography by Low Energy Electron Diffraction: Theory, Computation and Structural Results: Springer-Verlag: New York, 1979.

3. J. B. Pendry, "Low Energy Electron Diffraction", Academic Press, New York, 1974.

4. P. J. Rous and J. B. Pendry, Surface Science 219(1989) 355.

5. P. M. Marcus and F. Jona, eds., Determination of Surface Structure by LEED, Plenum Press, New York (1980)

6. G. Ertl and J. Kuppers, Low Energy Electrons and Surface Chemistry, Verlag Chemie, Weinheim (1974).

7. J. R. Creighton, K. M. Ogle, and J. M. White, Surf. Sci. 138(1982)L137.

8. S. M. Davis, F. Zaera, B. E. Gordon and G. A. Somorjai, J. Catalysis 92(1985)240.

9. M. Abon, J. Billy and J. C. Bertolini, Surf. Sci. 171(1986)L387.

10. N. Freyer, G. Pirug, and H. P. Bonzel, Surf. Sci. 126(1983)487.

11. R. Yu and T., Gustafsson, Surf. Sci. 182(1987)L234.

12. F. Masson, C. S. Sass, O. Grizzi, and J. W. Rabalais, Surf. Sci. 221 (1989) 299.

3.2. Auger Electron Spectroscopy

A second analytical technique which takes advantage of the inherent surface sensitivity of electron based techniques is Auger electron spectroscopy. Named in honor of Pierre Auger who discovered the effect incidentally to his Wilson cloud chamber studies of early particle physics, Auger electron spectroscopy is the most commonly used technique for elemental surface analysis [1]. Auger correctly surmised that the source of the tracks in his cloud chamber which did not change length, i. e. energy, despite changes in the energy of the ionizing radiation arose from those secondary electrons ejected as a result of internal electron re-arrangements within the affected atom. The theoretical basis for the Auger process became rapidly established during the 1920's and 1930's allowing cross sections to be accurately calculated not for their own purpose but only as a necessary correction to fluorescence measurements. At that time, the atomic physics community viewed Auger transitions only as a parasitic process to the main reaction of interest. Only years later did the Auger effect come into its own as a special technique for chemical analysis.

Auger electrons are produced by the process shown in figures 3.2(a) and (b). After the formation of a core level vacancy, usually by highly energetic electrons or photons, a non-radiative rearrangement may take place in which this vacancy is filled by a less tightly bound electron. This is followed by the ejection of a second electron bound by an energy less than the difference in

the energies of the first two electrons. The energy of the ejected electron is approximately given by

$$E_{AUGER} = E_K - (E_{LI} - E_{LII})$$

For example consider the Auger process for the oxygen atom whose energy levels are shown in the following diagram.

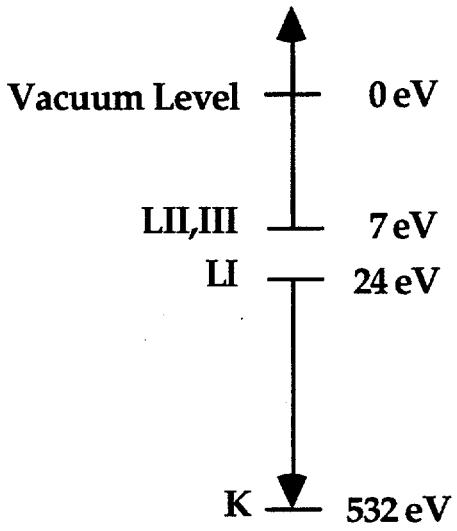

Figure q. Oxygen atomic energy diagram indicating energy levels involved in KLL Auger transition.

From this diagram the kinetic energy of the ejected electron would be given by

$$E_{AUGER} = 532 - 24 - 7 = 501 \text{ eV}$$

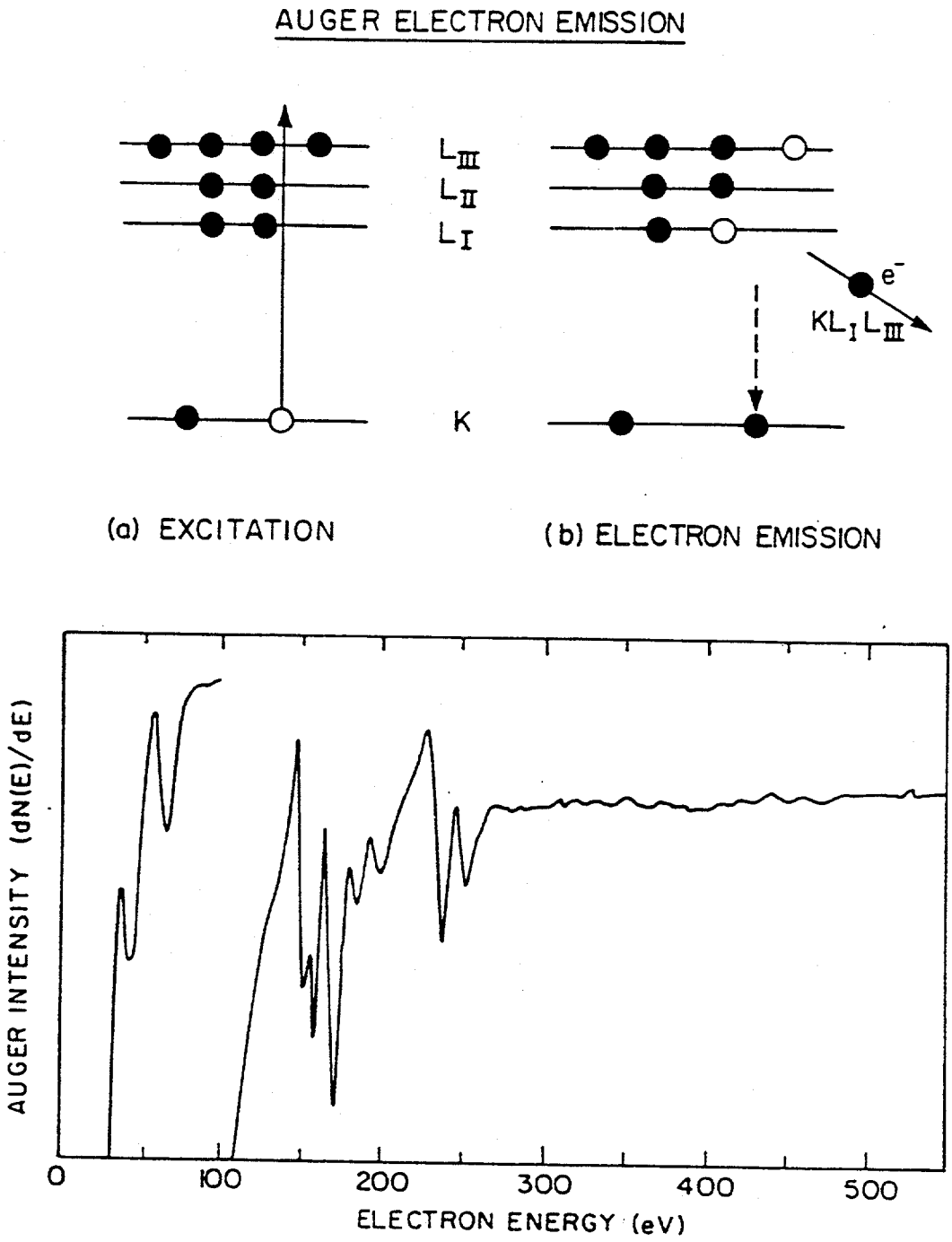

Figure 3.2. **The Auger process and the resulting Auger spectrum of a Pt surface.**

For this example , this estimate is excellent when one considers that the binding energy of the LI level has not been corrected for neither the presence of the vacancy in the L level nor the effects of coupling between the two unfilled shells in the final state.

The first suggestion that the Auger process could be used for surface analysis was made by Lander in 1953 [2]. AES became a viable tool for surface analysis after Harris published a short communication in which he demonstrated that by electronically differentiating the broad electron energy spectrum emanating from a metal surface bombarded by a high energy electron beam, he was able to make the small loss features arising from Auger transitions appear as distinct peaks on the slowly varying secondary background [3]. The electronic differentiation was accomplished by superimposing a sinusoidal wave form of a few volts in peak to peak intensity on the retarding potential of an electrostatic energy analyzer. By detecting only that fraction of the signal which appears at the superimposed frequency by means of a phase sensitive lock in amplifier, the first derivative of the N(E) vs. E spectrum is obtained. Shortly thereafter, Weber and Peria and others showed that the conventional three grid retarding field analyzer used for low energy electron diffraction studies could be similarly modified by phase sensitive detection at twice the superimposed frequency, making this technique a low cost add on to existing experimental apparatus [4,5]. Researchers could now quantify the degree of cleanliness of the surfaces that they had been observing LEED patterns and relate the additional ordered overlayer patterns to the identity of the adsorbate.

While today the vast majority of AES users enjoy the convenience, higher sensitivity and increased speed of AES using cylindrical mirror or

hemispherical analyzers, all the AES measurements used in this study were performed in the manner of Weber and Peria with the same four grid retarding field analyzer used for low energy electron diffraction studies.

There are two principal uses for AES in this study. Fundamental to all studies of surfaces is the determination of the extent of surface contamination. Quantitative coverage measurements are possible [6-13]. The changes in Auger signal intensity expected from typical idealized overlayer structures has been modeled by Gallon [14]. A modification of the Gallon procedure has been used by Biberian and Somorjai to calibrate the coverage of carbon overlayers on platinum [15]. Carbon overlayers were obtained by the decomposition of CO at elevated temperatures. A plot of the substrate Auger peak intensity against the adsorbate Auger peak intensity shows a distinct break in slope at the completion of a monolayer coverage. The corresponding ratios of the carbon 272 eV Auger peak intensity to the platinum 64 eV or 237 eV Auger peak intensity are 0.08 and 3.2 respectively. Two earlier values for the ratios of the carbon 272 eV Auger peak intensity to the platinum 237 eV Auger peak intensity not cited by these authors were 4 and 3.9 [16,17]. Additional ratio values corresponding to coverage of 0.25 monolayer were reported as 0.6 and 0.7 [17,18]. These values were obtained using a four grid LEED optic similar to those used in this study and were used to calibration coverages without modification. Had more precise calibration been desired, corrections to compensate for the differing line shapes as a function of coverage and temperature would have most likely have been necessary [18,19].

In addition to quantitative coverage measurements, studies of hydrocarbon adsorption studies can use AES to obtain chemical state information on the carbon or carbonaceous layer formed by hydrocarbon decomposition on metal surfaces. Auger transitions involving valence bands might be expected to display chemical shifts as the environment - valence or coordination - is changed. Few elements, however, display the large changes in line shape and positions as does carbon as they range from the characteristic "carbidic" features seen in metal carbides, isolated carbon atoms or amorphous carbon, and highly hydrogenated carbonaceous adspecies to the "graphitic" line shape belonging to elemental graphite, graphitic precipitates or deposits on the metal surface. Fundamental studies of the carbon auger line shape were performed on a series of gas phase hydrocarbon molecules [20]. The sensitivity of the Auger process to the local hybridization (sp^3, sp^2 or sp) was demonstrated by a comparison of the signature spectra of methane, ethylene and acetylene. The insensitivity of the Auger process to substituent effects was demonstrated by a comparison of the spectra obtained from a series of normal alkanes, methanol and acetone. In this latter case, the C $_{KVV}$ line shape retained sp^3 features regardless of the adjacent functional group. Upon chemisorption, these molecules show little change in the Auger line shape. In a crude sense, the Auger signature of the carbonaceous adlayer can be used to distinguish between those carbon deposits which are immediate catalytic poisons leading to catastrophic failure and those partially hydrogenated species with slow but measurable rehydrogenation rates that form the stable "steady state" carbonaceous overlayer on or among which the catalysis proceeds at a nearly constant rate.

3.2.1. References

1. P. Auger, Surf. Sci. 48 (1975)1.
2. J. L. Lander, Phys. Rev. 91 (1953) 1382.
3. L. A. Harris, J. Applied Physics 39(3), (1968) 1419.
4. R. E. Weber and W. T. Peria, J. Applied Physics 38, (1967) 4355.
5. R. E. Weber and A. L. Johnson, J. Applied Physics 40(1), (1969) 314.
6 M. P. Seah, Surface Science 32 (1972) 703.
7. C. D. Wagner, L.E. Davis and W. M. Riggs, Surf. Interface Anal. 2,(1980) 53.
8. J. C. Ashley and C. J. Tung, Surf. Interface Anal. 4, (1982) 53.
9. C. J. Powell, Scanning Electron Microscopy 4 (1984) 1649.
10. M. P. Seah and W. A. Dench, Surf. Interface Anal. 1,(1979) 2.
11. P. W. Palmberg and T. N. Rhodin, J. Applied Physics 39, (1968) 2425.
12. F. N. Palmberg, G. E. Riach , R. E. Weber and N. C. MacDonald, Handbook Of Auger Electron Spectroscopy, Physical Electronics Ind., Minnesota, 1972.
13. T. E. Gallon, Surface Sci. 17 (1969) 486.
14. J. P. Biberian and G. A. Somorjai, Applications of Surface Sci. 2 (1979) 352.
15. D. W. Blakely, Lawrence Berkeley Laboratory Report #LBL-6064, (1976).
16. R. M. Lambert, W. H. Weinberg, C. M. Comrie, J. W. Linett, Surface Sci. 27 (1971) 653.
17. J. C. Hamilton, Thesis Cornell University Ithaca N. Y. (1979).
18. G. Ertl and J. Kuppers, Low Energy Electrons and Surface Chemistry, Verlag Chemie, Weinheim (1974).
19. L. N. Tharp and E, J. Scheibner, J. Applied Physics 38, (1967) 3320.

3.3. High Resolution Electron Energy Loss Spectroscopy

High resolution electron energy loss spectroscopy provides information about the vibrational modes of adsorbed species [1-5]. From the frequency and number of bands, the structure of the surface bonds can be inferred. In these respects HREELS appears similar to conventional or surface infrared spectroscopy. The major advantages of electron energy loss spectroscopy include high sensitivity, ease of data acquisition and wide spectral range. One of the two vacuum chambers used in this work contained the HREEL spectrometer that is more completely described in earlier publications. Here, some background of the technique and the spectrometer will be described as it applies to this work.

When a monoenergetic beam of electrons is directed towards a solid surface, most of the electrons will scatter elastically. Some, however, will interact with the vibrational modes of the adsorbates, losing a quantum of energy equal to the energy of the particular vibration excited. A high resolution energy analysis of the scattered beam will identify that fraction of the electron beam involved yielding the vibrational spectrum. Additional information can be obtained through angular resolved measurements because of the selection rules derived from the details of the mechanism of the interaction.

The dominant mechanism of interaction is dipole scattering. Long range scattering at distance of 10 to 100 angstroms from the surface is due to

the interaction of the electric field of the incoming electron with the dynamic dipole of the vibrational mode of the adsorbed specie. Because the dynamic dipole of the vibrational mode of the surface species sets up a corresponding image dipole in the near surface region of the metallic substrate, only those vibrations or components of the vibrational mode perpendicular to the surface will interact with the incoming electron wave. Those vibrational modes parallel to the surface will have their dynamic dipole moment canceled or screened by the corresponding image dipole (Figure 3.3). This is the same mechanism which operates in infrared absorption and so the same selection rule applies. Dipole scattering is characterized by a scattered electron distribution peaked in the specular direction, falling off rapidly as the detector is moved away from the specular.

The other important type of interaction is the short range impact or resonance scattering. Here the incident electron interacts directly with the atomic potentials of the adsorbate. In the extreme case, it can be thought to be temporarily captured to form a negative ion. All vibrational modes can be excited by this mechanism. Because of the short range nature of this interaction the scattered distribution is isotropic. Only a small proportion of this distribution will be detected close to the specular direction. Spectra taken in the specular direction will be dominated by the electrons which interact by the dipole mechanism. Direct scattering modes can be distinguished from dipole scattering modes by the insensitivity of the intensity of the vibrational loss peak to detector positions away from the specular.

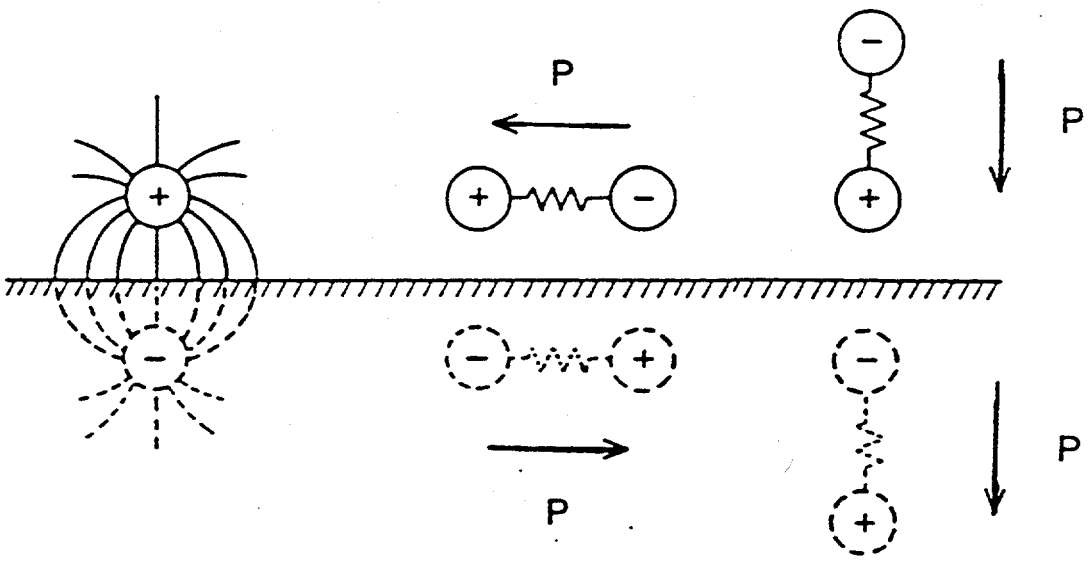

Figure 3.3. The dipole selection rule

The spectrometer used in these studies was of the 127 degree cylindrical electrostatic deflector type patterned after the design of Froitzheim and Ibach and constructed here at the Lawrence Berkeley Laboratory as was the special high stability low noise power supply for the filament and lens elements (Figure 3.4) [2]. Electrons emitted from a directly heated filament are focused by an Einsel lens onto the entrance slit of the monochromator to provide the monoenergetic beam of electrons of energy between 1 and 10 eV impinging on the sample at the fixed angle of 60 degrees. The specularly scattered electrons are collected and energy analyzed by a similarly shaped analyzer (total scattering angle of 120 degrees). A channeltron electron multiplier is used to detect the energy analyzed electrons in the conventional pulse counting mode. All data was collected using a conventional X-Y recorder. Typical resolutions of 40 to 100 cm-1 could be obtained for signals consisting of elastic peaks of 104 to 106 counts per second and loss peaks of several hundred counts per second.

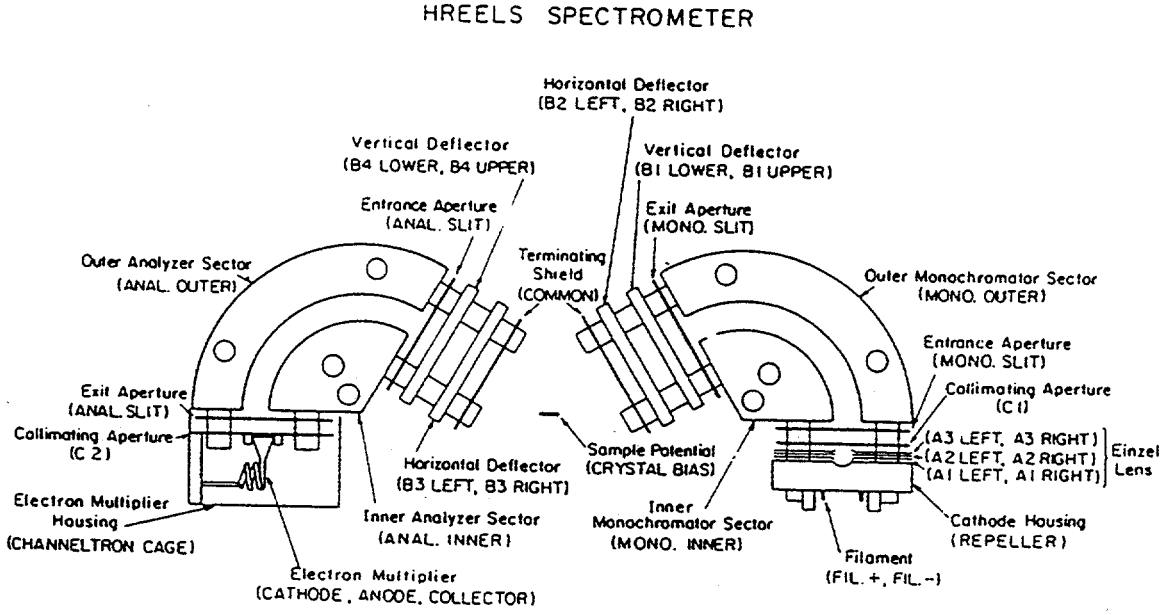

Figure 3.4. Schematic of the high resolution electron energy loss spectrometer.

3.3.1. References

1. G. Ertl and J. Kuppers, Low Energy Electrons and Surface Chemistry, Verlag Chemie, Weinheim (1974).

2. H. Froitzheim, H. Ibach and S. Lehwald, Rev. Sci. Instrum. 46(1975)1325.

3. H. Froitzheim, Electron Energy Loss Spectroscopy, in , Electron Spectroscopy for Surface Analysis, H. Ibach, ed., Springer-Verlag, New York, 1977.

4. H. Ibach and D. L. Mills, Electron Energy Loss Spectroscopy and Surface Vibrations, Academic Press, New York, 1982.

5. R. F. Willis, ed. , Vibrational Spectroscopy of Adsorbates, Springer--Verlag, New York, 1980

3.4. Temperature Programmed Desorption

No single technique is more frequently used to link fundament studies of chemisorption and surface reactions on well characterized ordered surfaces in ultra high vacuum environments with experimental results on industrial catalysts under industrial conditions than temperature programmed desorption or temperature programmed reaction studies [1-6]. The relevance is immediately appealing. By postulating that the rate limiting or even that a kinetically significant step of the reaction is either a desorption or a unimolecular decomposition, the surface scientist is able to isolate this step on a substrate with a sharply defined range of number and type of active sites and quickly obtain kinetic information for this fundamental reaction. Performed at its highest art, these techniques perform yeoman duties in providing parameters for kinetic modeling which mimic real life processes to the level of fundamental understanding. But the simplicity of the technique, the modesty of required equipment , and the ease of zeroeth level data processing also provides sufficient seduction leading to varying degrees of fallacious results.

Thermal desorption is a simple chemical reaction whereby adsorbed species break the surface chemical bond and are released into the gas phase in a unimolecular or a bimolecular process .

$$A_{(ads)} = A_{(g)}$$

$$A_{(ads)} + A_{(ads)} = A_{2(g)}$$

The rate of desorption and the molecularity of the desorption reaction is usually described in terms of a Polanyi-Wigner equation.

$$r_{des} = -dn_{(ads)}/dt = dn_{(gas)} = kN_{(ads)}^{x}exp(-E_d/RT)$$

From transition state theory, the so called "normal" values of the pre-exponential for fully mobile adlayers are approximately 10^{13} s^{-1} and 10^{-2} s^{-1} $molecule^{-1}$ cm^{-2} for first and second order desorption respectively.

The usual discussion of temperature programmed desorption begins with the Redhead paper and for the majority of the practitioners ends there. In this seminal paper on temperature programmed desorption under conditions of negligible re-adsorption, Paul Redhead derives for the reader an expression which relates the activation energy for desorption to the temperature at which the maximum desorption rate is observed through such variables as the linear heating rate, the surface coverage of adsorbate, and the kinetic order of desorption for the instances of first and second order desorption [2]. The key to the simplicity of the Redhead approach lies in the graphical demonstration of the independence of the value of the ln(b/v) term in the expression for a reasonable range of heating rates and pre-exponentials. Using this approximation, the solution to the differential equation of desorption not only becomes tractable but downright simplistic. First order desorption activation energies for a known coverage can be obtained from a single experiment!

Many papers have appeared since 1965 extending and refining this mathematically and mechanically simple technique. Most noteworthy are the approaches which directly address the weaknesses of the Redhead method, that is the singularity of the pre exponential and lack of coverage dependent parameters and/or the failure to address the compensation effect of pre-exponential and activation energy, the failure to ensure that a "vacuum" environment does not necessary imply "re-adsorption free " conditions, as well as those papers which espouse the view that more experiments yield more and better data.

An instructive eample to sway the novice Redhead user draws upon the presumption of the compensation effect to demonstrate a non intuitive result. It will use the data from a recent paper on TDS which compares theperformance of several computational methods, including the the Redhead equation, for evaluating simulated thermal desorption spectra [7].

COVERAGE (monolayers)	PRE-EXPONENTIAL (s^{-1})	ACTIVATION ENERGY (kJ mol^{-1})	PEAK TEMPERATURE (K)
0.0	$1 X 10^{12}$	100	340
0.5	$1 X 10^{13}$	95	350
1.0	$1 X 10^{14}$	90	360

The model system simulates the existence of pair-wise repulsive interactions between the adsorbates by assuming that the desorption energy varies linearly with the coverage from an initial value of 100 kJ mol^{-1} to a final value of 90 kJ mol^{-1} at saturation. They further assume that a compensation effect takes

place between the pre-exponential and the activation energy. While the focus of the paper is on the comparative results obtained by the different computational methods, one observation is relevant here. For the model system, the activation energy **decreases** with increasing coverage. As a result of the compensation effect between the pre-exponential and the activation energy, what is observed is an **increase** in peak temperature with increasing coverage. While the error in the absolute value would be less than 5% than the actual value a single valued pre-exponential based Redhead type analysis, would lead one to report an erroneous **trend** in the dependence of activation energy on coverage as well as the fundamental nature of the adsorbate-adsorbate interaction.

3.4.1. References

1. S. J. Lombardo and A. T. Bell, Surf. Sci. Reports 13(1991) 3.
2. P. A. Redhead, Vacuum 12(1962)203.
3. C. M. Chan and R. Aris and W. H. Weinberg, Appl. Surf. Sci. 1(1978)360.
4. D. A. King, Surf. Sci. 47(1975)403.
5. J. L. Falconer and R. J. Madix, J. Catal. 48(1977)262.
6. G. Ertl, Kinetics of Chemical Processes on Well-defined Surfaces, Catalysis-Science and Technology, vol. 4,J. R. Anderson and M. Boudart eds., Springer-Verlag, 1983.
7. A. M. de Jong and J. W. Niemantsverdriet, Vacuum 41(1990)232.

3.5. Reaction Studies on Model Crystal Surfaces

Reaction studies performed on well characterized metal surfaces have become a routine procedure in the surface science of catalysis. While the procedures and rationale have not been significantly altered since the first experiments by Peterson and Somorjai, the variety and number of such system have grown significantly [1]. Recent reviews of catalytic reactions using single crystal metal surfaces describes some dozen classes of reactions that have been studied (Table 3.2) [2,3]. Excellent agreement has been obtained between studies on these single crystal surfaces and studies on supported metal catalysts demonstrating the relevance of the use of these systems to model the behavior of industrial catalysts. Commercially manufactured reactor systems are now also available.

By isolating the sample, either a foil or slice of single crystal material, from the ultra high vacuum environment , through raising the tubular portion of the lower half of the reactor manifold to meet the upper half in a modified Conflat seal, an effective batch reactor is created without destroying the integrity of vacuum of the bell jar (Figure 3.5). The requirement of the reactor volume to be well mixed is met by the use of an external positive displacement bellows type recalculating pump. All wetted parts of this pump are constructed of perflouropolymeric material to avoid untoward metal catalyzed reactions. The volumetric pumping speed of this pump is

Table 3.2. Examples of reactions that have been studied using single crystal metal substrates.

Ammonia synthesis	Ethylene epoxidation
CO oxidation	Thiophene hydrodesulfurization
Alkane hydrogenolysis	Alkane isomerization and cyclization
Olefin hydrogenation	Acetylene cyclotrimerization
Water-gas shift reaction	CO methanation
Methanol synthesis	

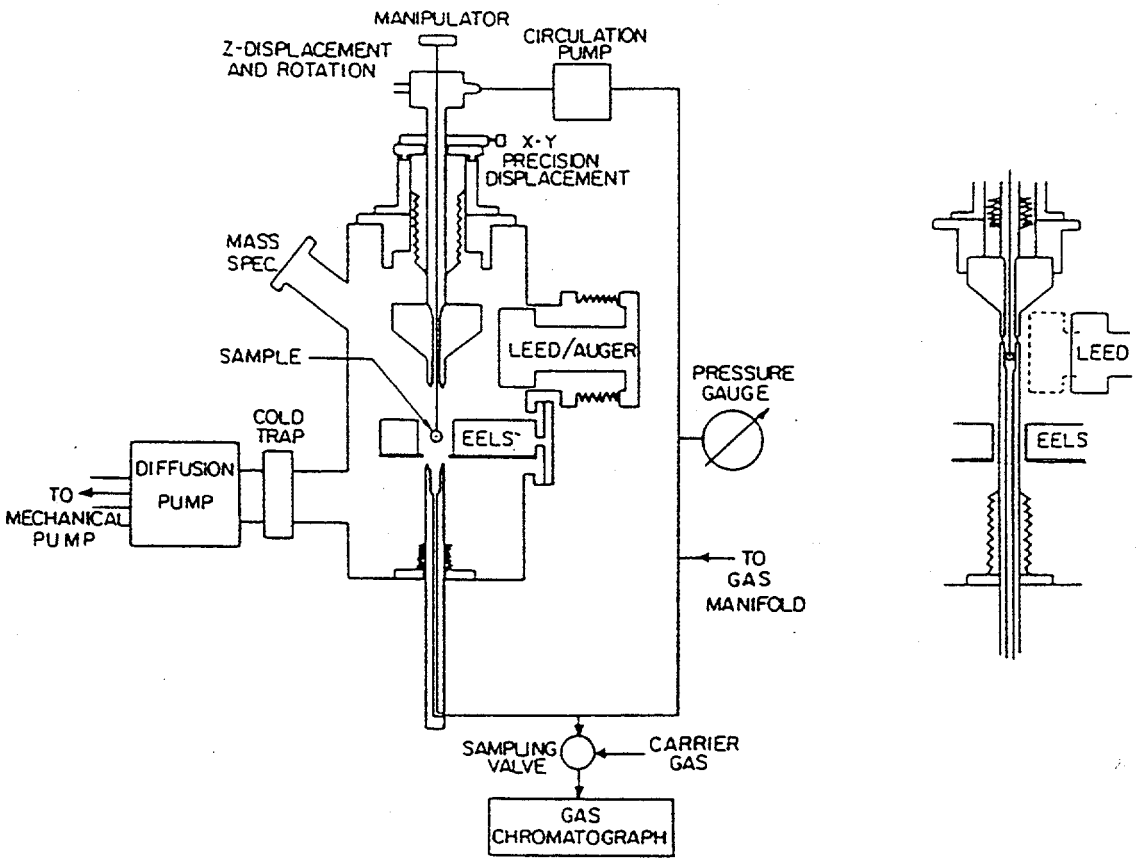

Figure 3.5. HREELS chamber with high pressure cell.

approximately 500 cc min^{-1}, or 0.75 reaction volumes min^{-1}. The major resistance in the flow system is that of the gas sampling valve associated with the gas chromatograph. Had greater mixing efficiency been necessary, this valve could have been by-passed in such a manner that it would have been re-introduced into the flow path only immediately prior to sampling. The use of premixed reaction gas mixture and sampling times greater than the reaction volume mixing time simplified the reactor system

A batch reactor is a type of reactor that is filled with reactants at some initial time and then operated as a closed system except for heat flow. Some type of mixing must be provided to maintain the system in a well mixed state to avoid temperature or concentration gradients within the reaction zone. Reaction product concentrations are allowed to build up as the contact time progresses. For many of the reactions studied, this is the only way of increasing the product concentration to the detection limit of the chromatograph. Other reactor types such as the continuous stirred tank reactor or the plug flow reactor have not been used with single crystal substrates.

Because of the small number of possible active sites (~10^{15}) many reactions proceed to less than 10% conversion and the kinetics are evaluated under these initial conditions. However facile reactions such as olefin hydrogenation can be monitored and evaluated at conversions in excess of 90%. Because not all reactions are the trivial case of zero order or pseudo-zero order kinetics, it is instructive to describe in more detail the expected relationships between reaction time and extent of conversion for the batch reactor type [4,5].

The descriptive equations for the various ideal reactors come from the application of a mass balance over the whole or differential part of the reactor.

rate of accumulation of A in the reactor =
(rate of flow of A in) - (rate of flow of A out)- (rate of disappearance of A by reaction)

For the well mixed batch reactor, this simplifies to

$$(r_A)\, V_r = dN_A/dt$$

where:

N_A = total number of moles of A in the reactor

Vr = the reactor volume

r_A = the rate of reaction.

the rate of reaction is usually expressed as a power law

$$r_A = k[A]^n$$

since the number of moles of A at any time can be related to the initial concentration by the fractional conversion XA, the mass balance can be rewritten as

$$dt = -(NAi)\ dXA/-(rA)\ Vr$$

or

$$t = \int_0^{X_{AF}} \frac{-N_{AI}dX_A}{(-r_A)V_r}$$

This is the design equation for a batch reactor applicable for all order of reactions. For the cases of a first order or second order, isothermal, constant volume reaction, this equation simplifies to

$$t = -(1/k)\ \ln[1-XA]$$

and

$$t = V_R/k\ N_{Ai}\ \{X_{Af}/(1-X_{Af})\}$$

respectively.

3.5.1. References

1. D. R. Kahn, E. E. Petersen and G. A. Somorjai, J. Catal. 34 (1974) 294.

2. J. A. Rodriguez and D. W. Goodman, Surface Sci. Reports 14 (1991) 1.

3. C. T. Campbell, Adv. Catal. 36 (1989) 1.

4. J. M. Smith, Chemical Engineering Kinetics, McGraw-Hill, New York, 1981.

5. O. Levenspiel, Chemical Reaction Engineering, John Wiley and Sons, New York, 1962.

3.6. The Rational Basis for Preparing Clean Metal Surfaces

Recipes and anecdotes for the preparation of clean single crystal metal surfaces form the obligatory initial chapter in most of the theses emanating from research groups involved in surface science studies. A compilation of such cleaning techniques has appeared in the literature to aid the researcher. While the concepts of surface segregation, bulk solubility, precipitation and surface reaction are adequately defined in these works, quantitative information regarding the thermodynamics of segregation and solubility and the kinetics of bulk diffusion and surface reaction are often missing or poorly understood. Bulk non-metallic impurities such as boron, carbon, sulfur and chlorine are often lumped together in qualitative discussion of solubility and segregation as if the magnitudes let alone the sign of enthalpies of these processes were the same! The use of gaseous reactants to remove surface contaminants is described without attention to the gas-surface and gas-bulk equilibria that is established. Often reaction products are not stated nor is any attempt made to verify and monitor the proposed reaction. While it is true that high temperatures and long times is often the answer to the questions of sample preparation, it is the intent of this section to address the thermodynamic and kinetic considerations underlying this intuitive approach. The goal of this introspection is to gain an understanding of the chemistry behind the cleaning procedures that are so widely used. One specific systems that will be described in detail is boron in rhodium.

Let us begin by describing a system consisting of a thin slice of metal containing a single bulk non-metallic impurity held at an elevated temperature in the static ultra high vacuum environment and attempt to describe the processes which may take place as the surface is exposed to a reactive gas in the typical cleaning procedure. Prior to the introduction of the reactive gas, the impurity in the metal has been distributed throughout the bulk of the crystal as a solute, on the surface of the metal as a segregated phase and in the vapor phase together with some partial pressure of gaseous metal atoms as would be appropriate for a solution with some degree of regularity. Compound formation of bulk or surface phases is also possible in some systems with their corresponding bulk-surface-gas equilibria. The bulk-surface and gas-surface equilibria as well as the solid state reaction equilibrium are of course established only in the absence of kinetic restraints.

Many of the reactions to consider are given in the following Table 3.3. The corresponding energy level diagram is shown in Figure 3.6. Although the intent is to illustrate the most general case of a metal-impurity system, already some important specific relationships are demonstrated. For instance, the impurity is shown to have an endothermic heat of solution, that is, the solubility increases with temperature. This is not true for all impurities. Also the heat of segregation is shown to be a positive quantity. For this system the equilibrium surface coverage increases with temperature. Again this is specific for this hypothetical system and not true for all impurities.

Considerations of impurity concentration and experimental temperature ranges will allow us to eliminate the reactions of least significance. The minimal data required is the M-I phase diagram and a table of vapor pressures for M, I and MI at the temperature of interest. The role of

bulk compound formation is directly assessed by consulting the phase diagram. Metal which easily form bulk carbides and sulfides should be expected to retain these impurities through the sample preparation procedure and therefore should be more difficult to clean. Iron is an excellent example of a base metal which forms carbides and sulfides over a wide range of compositions [2] and which has a notorious reputation as a difficult to clean material. Platinum on the other hand is predicted not to form the carbide phase, and hence has a low solubility limit, which makes it a relatively easy material to effectively clean. Normally, the process of producing the pure metal sample (zone refining or electrodeposition) has reduced the bulk impurity to levels far below that required for compound formation. However it is possible to inadvertently increase the impurity concentration in the near surface region during experimentation, such that bulk compound phase boundaries may be exceeded (vide infra). Surface phase compound diagrams have not been widely explored except for the work of Oudard who established the thermodynamic stability of surface metal sulfide phases. These phases are in general approximately 20% more stable than the corresponding bulk phases. An empirical correlation of the free energies of formation of surface and bulk sulfides and halides show this to be a general trend.

Having established the number and type of bulk and surface phases expected to be present, it is now necessary to determine the role of gaseous species. The volatility of the impurity phase or a reaction product thereof may play a key role in deciding a strategy for its removal. The evaporation rate of the metal sample and or its melting point establishes the experimental upper temperature limit. Vapor pressures of non-metallic impurities are can

be both higher and lower than the metal and the dependence of the equilibrium vapor pressure of a pure substance on temperature is given by the Clausius-Clapeyron equation.

There are three processes to remove impurities from the near surface region:

1. Sublimation or vaporization
2. Reaction with an added gas to form a volatile product
3. Physical removal by sputtering processes

Temporary accumulation of an impurity in the near surface region in excess of the bulk concentration may be re-distributed throughout the bulk by annealing to high temperatures may reduce the surface coverage to low levels, but does not *clean* the sample in the sense used here. A typical example of this procedure is the practice of flashing a platinum sample to high temperatures following hydrocarbon adsorption to reestablish a clean surface for additional studies.

Table 3.3. Important chemical reactions occurring during sample preparation

1.	$I_{bulk} = I_{ads} = I_{gas}$	bulk-surface-vapor equilibrium
2.	$M_{solid} = M_{gas}$	solid-vapor equilibrium
3.	$M_{solid} + I_{solid} = MI_{bulk}$	bulk compound phase formation
4.	$MI_{bulk} = MI_{ads} = MI_{gas}$	bulk-surface-vapor equilibrium
5.	$MI_{bulk} = M_{bulk} + I_{gas}$	incongruent evaporation
6.	$M_{solid} + I_{ads} = MI_{ads}$	surface compound phase formation

where M = metal, I = non-metallic impurity and ads = adsorbed surface phase

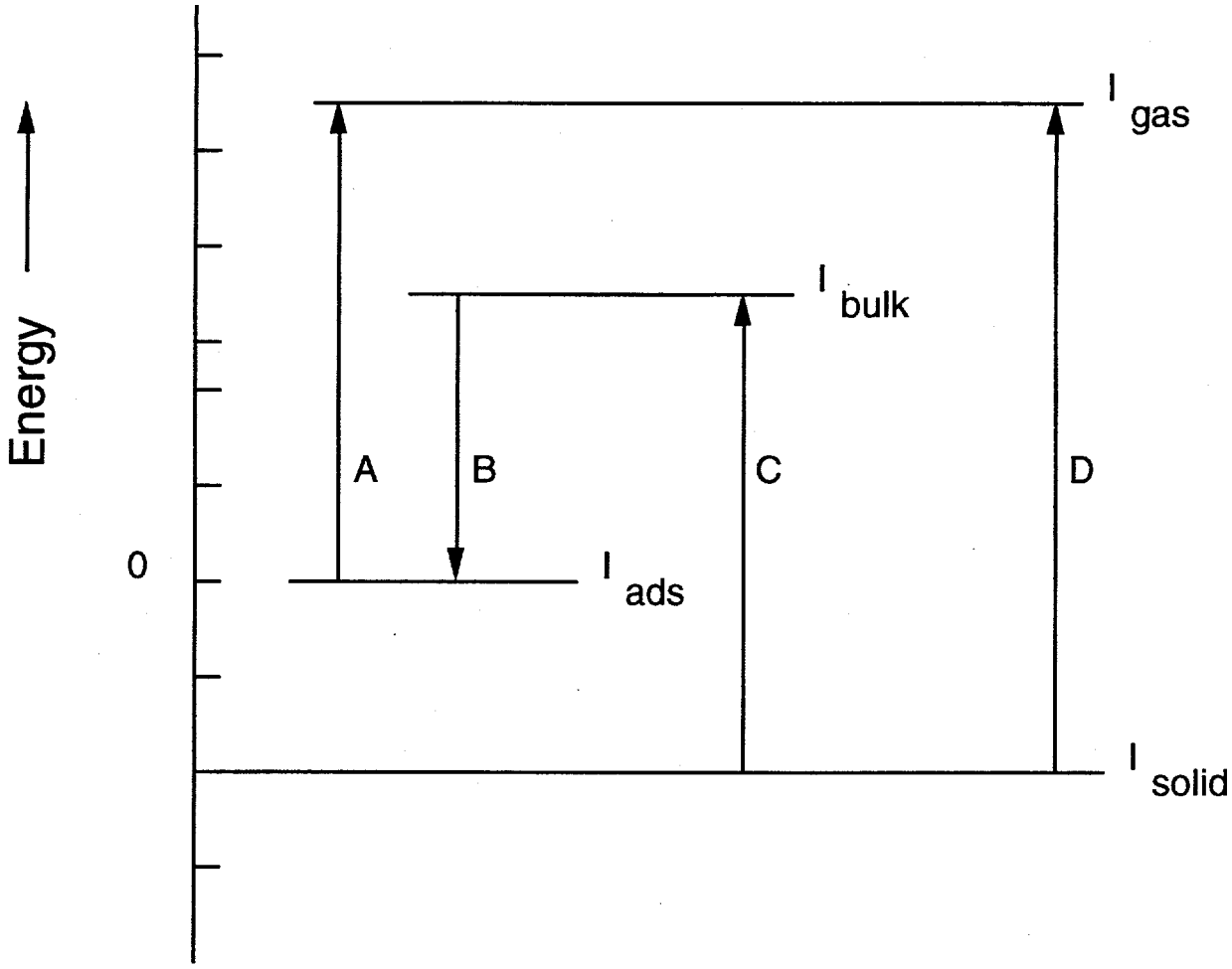

A- Surface Binding Energy

B- Energy of Segregation

C- Energy of Solution

D- Energy of Vaporization

Figure 3.6. Hypothetical energy level diagram for a non-metallic impurity I within metal M.

Let us examine in detail the cleaning procedure for the most recalcitrant of the impurities systems encountered in this work, namely boron in rhodium. The effect of boron on rhodium surface adsorption and reactivity has been previously reported, but not studied as an example of a segregation process [3-5]. The bulk phases Rh_2B (4.99 wt.% B), RhB (9.51 wt.% B) and a phase higher in boron content than RhB_2 are known to exist [2]. As had been previously postulated, it is no surprise that this contaminant be found at high concentrations following the zone refining process. The small size of the boron atom allows easy interposition within the rhodium lattice as an interstitial impurity much like carbon in nickel. Unlike the geological origin of many of the impurities found in the metals of interest, the origin of boron is anthropogenic in nature, being ascribed to contamination of the metal by the boride crucible used during the sample preparation stage. Heating the sample in vacuo is not sufficient to remove the boron through the process of sublimation. The generally recommended cleaning procedure is to first heat the sample in 10^{-7} torr O_2 at elevated temperatures to fix the boron on the surface as the oxide. This part of the procedure is effective due to the extreme low solubility of the boron oxide in rhodium compared to boron. Once the contaminant is immobilized on the surface, it is said that the layer can be effectively sputtered off the surface by routine noble gas sputtering procedures at moderate potentials, 0.5 to 1.5 KeV. In reality, boron and/or boron oxide can be resistant to such treatment and requires prolonged repetitive cycles of oxide fixation, ion bombardment and thermal annealing on the order of tens of hours for each step of the system. Figure 3.7 illustrates the typical Auger spectrum for a saturated layer of boron oxide on the rhodium surface. Under the conditions used for the Auger spectroscopy (2.0

keV primary energy, 8 V p-p modulation, near grazing incidence, RFA detection) the Auger signature is marked by a pronounced doublet near 168 and 178 eV caused by the substantial contribution of the boron to the poorly resolved rhodium transitions in that region. Even more indicative of a high coverage of boron oxide is the presence of oxygen transitions where O_{510}/Rh_{302} ratios reach approximately 0.061 for the saturated layer. LEED observations performed on this overlayer show only a (1X1) pattern with no discernible extra spots. Oxygen adsorption on this overlayer causes a p(2X2) pattern to appear. Interesting enough, subsequent exposure of this oxygen saturated surface to a flux of carbon monoxide restores the (1X1) pattern. HREELS measurements at this point indicate that this surface is not capable of adsorbing carbon monoxide. The lesson to be learned from this anecdote is that boron in rhodium is not easily detected by Auger spectroscopy due to the overlap of the transitions in the 178 eV region. If the P-P modulation is increased in an effort to increase sensitivity, their will be a corresponding increased difficulty in judging quantitatively the amount of boron by judging the relative depths of the poorly resolved 168-178 eV doublet. On the other hand, the typical RFA detectors and electronics used in this study require a high (>6 V P-P) modulation to see any signal in the oxygen region. Generally, a surface was deemed "clean" when O_{510}/Rh_{302} ratios were 0.01 or less. One may ask, why is it necessary to remove the boron oxide by sputtering? Looking at the thermodynamics of vaporization for B_2O_3, it is tempting to conclude that removal of born oxide should be facile at high enough temperatures.

$$B_2O_3\ (l) \quad = \quad B_2O_3\ (g)$$

Temperature (K)	B_2O_3 vapor pressure (torr) [1]
800	1.4×10^{-14}
1000	2.5×10^{-9}
1300	1.4×10^{-4}

However, saturated coverages of boron oxide were observed to be stable at 1300 K in vacuum. Either the surface phases of boron oxide are considerably more stable than the bulk compound or kinetic limitations are present.

Could the boron be removed by reaction with additional oxygen as is the general case for dissolved carbon?

$$B_2O_3\ (l) + O_2 = BO_2(g)$$

The Gibbs free energy change for this reaction at 1300 K is +167kJ, so this is not an option under vacuum conditions.

Do we need fear disproportion of the oxide at elevated temperatures and prolonged times?

$$B_2O_3\ (l) = 2B + 3/2\ O_2$$

Temperature (K)	O_2 pressure (torr) [1]
1000	2.6×10^{-33}
1300	2.1×10^{-23}
1500	5.1×10^{-19}

Again, the thermodynamics predict that this is an unfavorable reaction for all realistic vacuum conditions.

While the solution to the problem of boron contamination encountered in this work required the Edisonian formula of long times at high temperatures, it is hoped that thoughtful consideration of the chemistry of sample preparation using available thermodynamic and phase diagram information will help future problems.

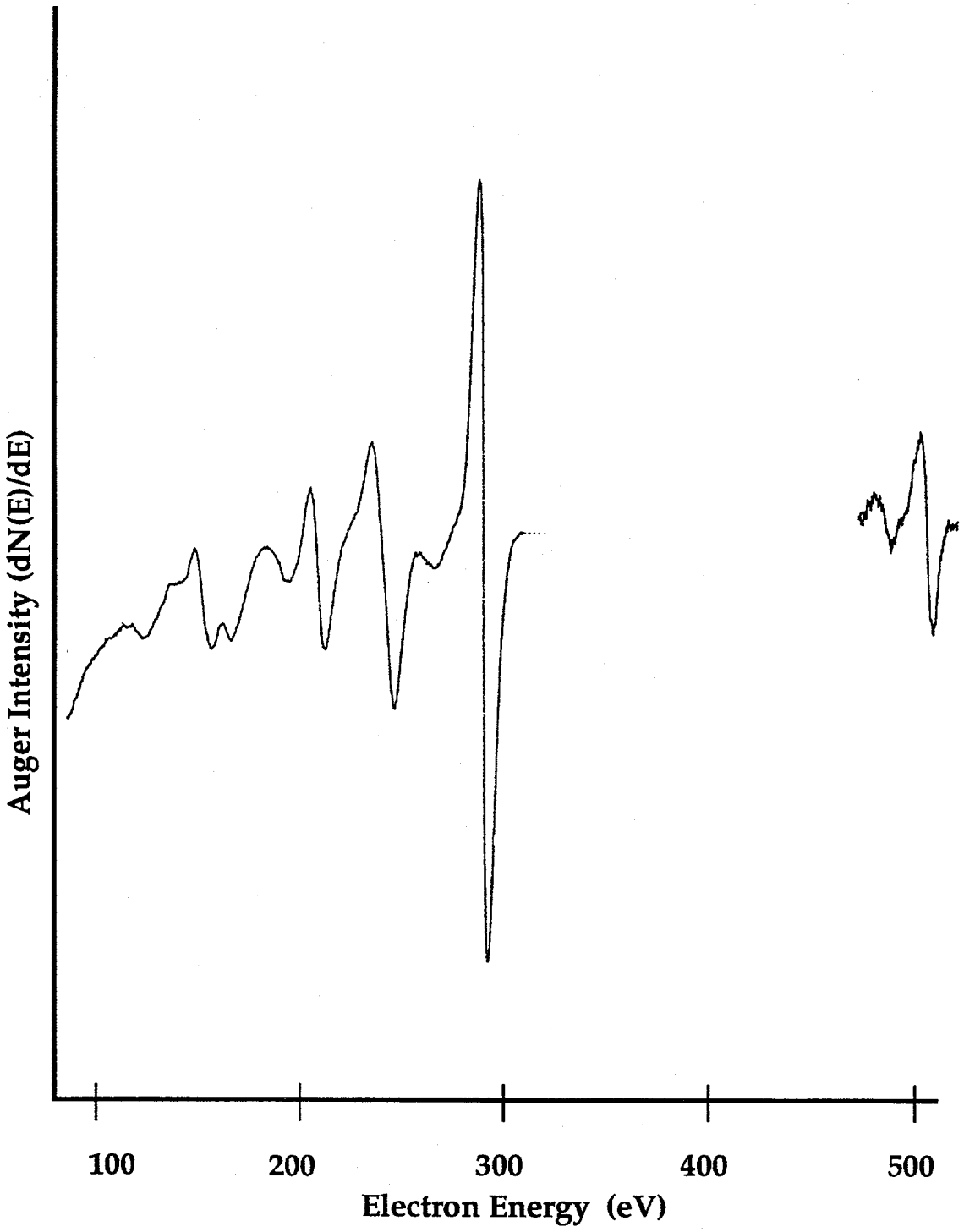

Figure 3.7. Auger spectrum of Rh(755) heavily contaminated with boron.

3.6.1. References

1. D. R. Stull and H. Prophet, JANAF Thermochemical Tables, 2nd ed., NSRDS-NBS 37, U. S. GPO, Washington D. C. , 1971

2. E. M. Levin, C. R. Robbins, and H. F. McMurdie, Phase Diagrams for Ceramists, Am. Ceram. Soc., Columbus, OH, 1964.

3. J. Kiss and F. Solymosi, Surf. Sci. 135 (1983) 243.

4. J. Kiss and F. Solymosi, Surf. Sci. 149 (1985) 17.

5. J. Kiss and F. Solymosi, Surf. Sci. 177 (1986) 191.

4. Experimental Results

4.1. Vibrational Spectroscopy Studies of Ethylene Adsorption on a Stepped Rhodium Surface

Vibrational studies of ethylene adsorption on a stepped rhodium surface were performed in order to assess the stability of ethylidyne on the stepped rhodium surface compared to previous studies performed on the Rh(111) [1] and Rh(100) [2] surfaces.

The Rh(755) crystal was cleaned by repeated cycles of heating from 500 to 1300K in 5 X 10^{-7} torr of oxygen, argon ion bombardment using 1.5 keV Ar^+ beams at ~5 microamps of current from sample to ground in 5 X 10^{-5} torr of argon, and prolonged annealing in vacuum at temperatures up to 1300K. Boron, carbon, oxygen and sulfur could be satisfactorily removed by this procedure. The cleanliness of the surface region was determined by periodically taking Auger spectra. LEED patterns obtained from this sample gave the characteristic hexagonal pattern of "split spots" as would be expected from a hexagonal substrate with periodic step arrays. The LEED optics used in this phase of the study exhibited severe distortions primarily due to the use of mismatched electron gun and retarding grid assemblies. Visual observations could be made only with great difficulty. Photographic recording of patterns was impossible. Only visual observations were recorded.

4.1.1. HREELS Study of Ethylene Adsorption at Room Temperature

After a cleaning procedure and the verification of surface cleanliness by AES and surface order by LEED, a saturation dose of ethylene was introduced to the surface at room temperature. The HREEL spectrum obtained is shown in figure 4.1(A).

The spectrum compares favorably with that obtained by room temperature ethylene adsorption on the Rh(111) and Rh(100) surfaces (Table 4.1). This species has been previously identified as the ethylidyne species through the combined use of TPD, HREELS, and LEED structure determinations [3,4].

The spectrum is characterized by the appearance of the vibrational modes of the various functional groups associated with the adsorbed ethylidyne species. The lowest vibrational frequencies belong to the metal-carbon stretching vibrations (<600 cm^{-1}). Carbon-carbon (900 - 1900 cm^{-1}) and carbon-hydrogen bending frequencies (700-1500 cm^{-1}) appear next. Finally one observes carbon-hydrogen stretching vibrations above 2800 cm^{-1}. The assignment of the rhodium-carbon stretch at 485 cm^{-1}, , the methyl symmetric and antisymmetric bending modes at 1350 and 1390 cm^{-1}, respectively, and the methyl stretching mode at 2930 cm^{-1} are in accordance with these usual functional group values. One difference may be the observed shift in the C-C stretching frequency from 1120 cm^{-1} on the (111) surface to 1070 cm^{-1} on the stepped surface, indicating a weakening of the C-C bond due to increased bonding with the surface. This may arise from interaction with the step. Similar shifts to lower wave numbers have been observed as a result of CO coadsorption on the Rh(111) surface [1]. An earlier investigation by the Winograd group [6] compared the relative coverage of

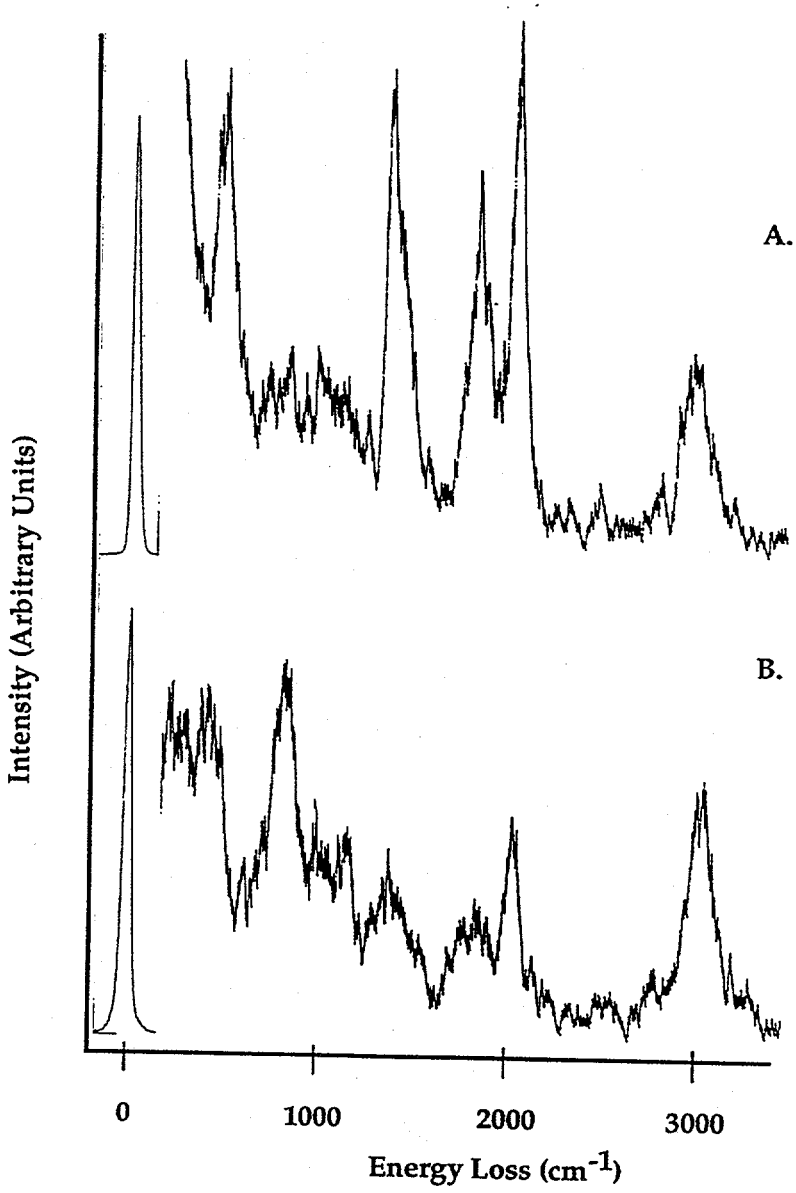

Figure 4.1. **(A) Specular HREEL spectrum of a Rh(755) surface following saturation dosing of ethylene at room temperature.**
(B) Specular HREEL spectrum of an ethylidyne overlayer on a Rh(755) surface after annealing to 500 K

Table 4.1 **Comparison of the vibrational frequencies (cm^{-1}) for ethylidyne on Rh(111) and Rh(100) surfaces with ethylidyne on the Rh(755) surface.**

Mode Description	Rh(111)	Rh(100)	Rh(755)
Rh-C	435	425	484
ρ CH_3	972		827
υ C-C	1121	1015	1070
δ_s CH_3	1335	1350	1350
δ_{as} CH_3	1420	1408	1390
υ_s CH_3	2880	2915	2930
Reference	[1]	[3]	this work

ethylidyne on the stepped Rh(331) surface to the Rh(111) surface. Using X-ray photoelectron spectroscopy (XPS), they demonstrated that the saturation ethylidyne coverage on the stepped surface was 80% of that of the (111) implying that the surface coverage scales with the number of three fold sites . No special reactivity or surface
binding states were associated with the presence of step sites, a result in agreement with this study.

The room temperature HREEL ethylidyne spectrum is also in good agreement with the infrared spectrum of ethylidyne obtained on an alumina supported rhodium catalyst (Table 4.2). The average metal particle size of 18 angstroms would be expected to provide a rough surface for chemisorption, much like the stepped surface used in this study. This particle size also falls within the range where reaction structure sensitivity is most apparent (10-50 angstroms). Again, by comparison, a lower C-C stretching frequency is found for the stepped surface.

4.1.2. HREELS Study of Ethylidyne Decomposition at 500 K

After heating the sample in vacuum to 500K and then cooling to room temperature, significant changes in the spectrum were observed (Figure 4.1(B)). Most apparent is the loss of features associated with methyl group vibrational modes indicating that dehydrogenation to CH or C_2H species has occurred. As a result, there is a shifting in the metal-carbon stretching frequency from 484 to 423 cm^{-1} as well as increase in the C-H stretch from 2924 to 3000 cm^{-1}. In addition, there is also a pronounced increase in the intensity

Table 4.2. Comparison of the vibrational frequencies (cm^{-1}) for ethylidyne on Rh/Al_2O_3 with ethylidyne on the Rh(755) surface.

Mode Description	Rh/Al_2O_3	Rh(755)
Rh-C		484
ρ CH_3		827
υ C-C	1110	1070
δ_s CH_3	1342	1350
δ_{as} CH_3	1408	1390
υ_s CH_3	2885	2930
Reference	[7]	this work

Table 4.3 **Comparison of the vibrational frequencies (cm^{-1}) for acetylide on Rh(111) and Rh(100) surfaces with that of the ethylidyne decomposition species on the Rh(755) surface.**

Mode Description	C_2H on Rh(111)	C_2H on Rh(100)	C_xH on Rh(755)
υ CH	3020	3025	3000
υ C-C	1380	1305	1371
combo Rh-C + δ CH	1170		1161
δ CH	815	805	827
υ_s Rh-C	490	430	423
υ_{as} Rh-C	not observed	370	
Reference	[1]	[3]	this work

Table 4.4. Comparison of the vibrational frequencies (cm^{-1}) for methylidyne on Rh(111) and in a ruthenium organometallic cluster compound with that of the ethylidyne decomposition species on the Rh(755) surface.

Mode Description	CH on Rh(111)	$H_3Ru_3(CH)(CO)_9$	C_xH on Rh(755)
υ CH	2930	2988	3000
combo Rh-C + δ CH	1170		1161
δ CH	740	894	827
υ_s Rh-C	not observed	670	423
υ_{as} Rh-C	not observed	427	
Reference	[1]	[4]	this work

of the out of plane δ CH deformation band observed at 827 cm^{-1}. These changes are very similar to previous observations made after annealing an adsorbed ethylidyne layer to approximately 500 K on both Rh(111) [1] and Rh(100) [2]. It is likely that dehydrogenation has occurred to the level of CH or C_2H species since the characteristic CH_2 scissors mode at 1000 and 1400 cm-1 are very weak or absent.

A comparison of the spectrum to that for the acetylide (C_2H) (Table 4.3) and methylidyne (CH) (Table 4.4) species on rhodium surfaces and in model organometallic compounds indicates that the acetylide species is the most probable majority species remaining on the stepped surface. The C-C bond appears to be still intact at this temperature. In this respect, no gross differences appear to exist for these three different rhodium surfaces on which ethylene adsorption and thermal decomposition has been investigated

4.1.3. References

1. B. E. Bent, Ph. D. Thesis, University of California, Berkeley (1986).
2. C.- T. Kao, Ph. D. Thesis, University of California, Berkeley (1988).
3. H. Ibach and D. L. Mills, Electron Energy Loss Spectroscopy and Surface Vibrations, Academic Press, New York (1982).
4. R. J. Koestner, M. A. Van Hove and G. A. Somorjai, Surf. Sci. 121(1982) 321.
5. M. W. Howard et al, J. Chem Soc., Faraday Trans. 2 77 (1981) 397.
6. R. Levis, N. Winograd, and L. A. DeLouise, J. Am. Chem. Soc. 109 (1987) 6873.
7. S. B. Mohsin, M. Trenary and H. J. Robota, J. Phys. Chem. 95 (1991) 6657.

4.2. Reaction Kinetics

The primary motivation for this work is to attempt to compare the relative reaction rate of ethylene hydrogenation on platinum and rhodium surfaces as well as to use surfaces of well defined but differing geometries so as to ascertain the presence of any structural sensitivity. To this end, results will be presented in the following order:

- Rh(755) and Rh foil
- Pt(111) and Pt foil

A typical product accumulation plot is shown in Figure 4.2. Because of the large excess of hydrogen used and the zero order dependence of the rate on the ethylene partial pressure, these plot showed excellent linearity up to approximately 90% conversion levels. The rate of reaction was calculated from the slope of the plot in all cases. Error limits calculated from the standard deviation of the slope were generally in the range of 5 to 20% of the reported value. The accuracy of the gas chromatographic analysis verified by standard calibration samples was better than 5%.

4.2.1. Rh(755) and Rh foil

A Rh(755) sample was prepared as previously described. The specimen was elliptical in shape and exposed a total surface area of 0.78 cm^2 on its faces.

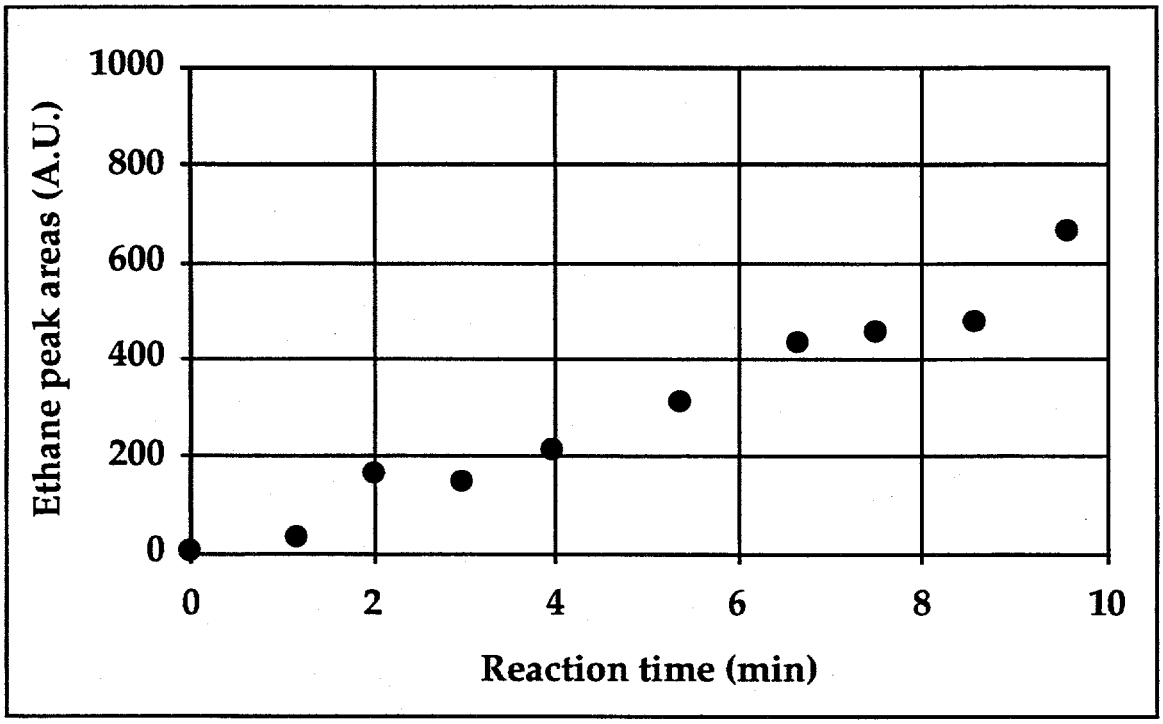

Figure 4.2. Typical product accumulation vs. reaction time plot

(Platinum foil; 77 torr ethylene; 723 torr hydrogen; total pressure 800 torr; 304 K)

The stepped surface was tested for activity over the temperature range of 300-400 K at a total pressure of 800 torr using two reactive gas mixtures, one consisting of 25 torr ethylene, 200 torr hydrogen, with the balance argon to achieve a total pressure of one atmosphere the other a premixed cylinder of 10% ethylene in hydrogen. The results are presented in an Arrhenius plot form in Figures 4.3 and 4.4. In each case an activation energy of 7 to 9 kcal mol^{-1} was calculated.

The accuracy of the results obtained using the 25 torr ethylene, 200 torr hydrogen mixture was limited since these results were obtained without the benefit of an integrator or a temperature controller. Accordingly, no attempt was made to determine the precise reaction order in either hydrogen or ethylene from these results. If one were to assume a zero order dependence in the olefin, a typical assumption for hydrogenation reactions, the resulting order in hydrogen would be between 1.0 and 2.0, again a typical result seen in the literature.

Multiple samples of 3 mil (0.008 cm) thick rhodium foil were cut in rectangular shapes and cleaned in the same manner as the single crystal samples. Samples areas ranged from 1.3 to 2.2 cm^2 . The surface was tested for activity over the temperature range of 300-400 K at a total pressure of 800 torr using a reactive gas mixture consisting of a premixed cylinder of 10% ethylene in hydrogen. The results are presented in an Arrhenius plot form in Figure 4.5.

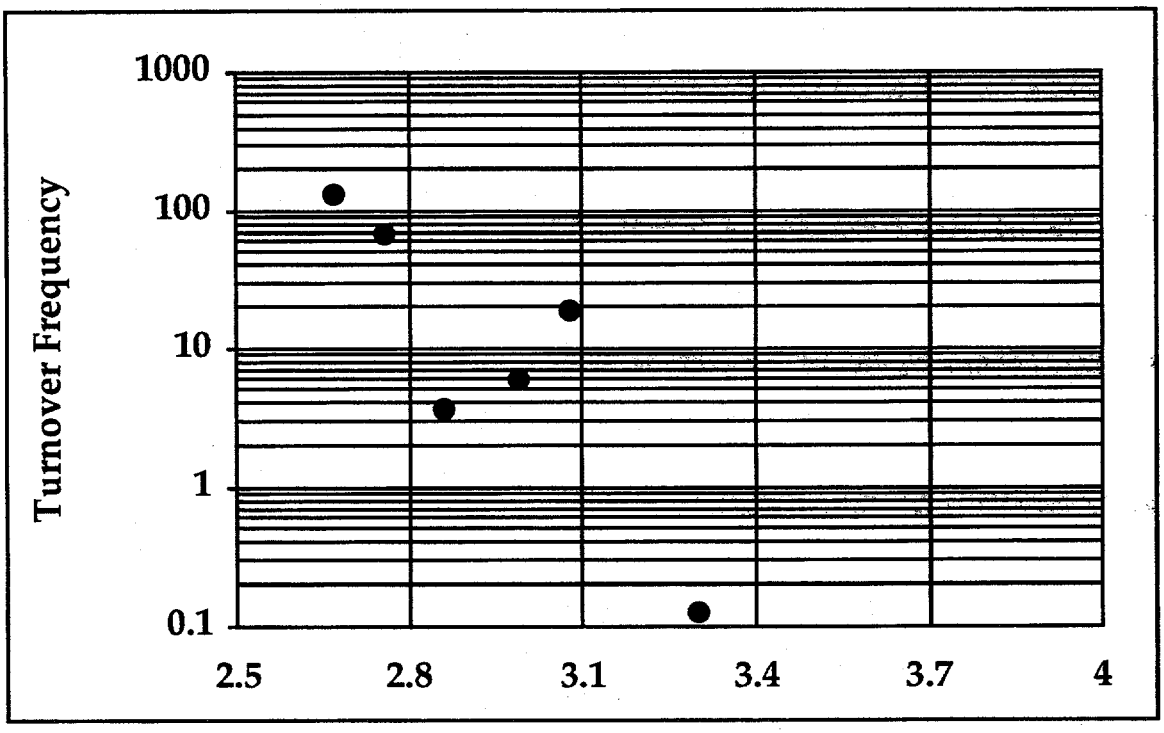

Figure 4.3. Arrhenius plot for ethylene hydrogenation on Rh(755)

(25 torr ethylene; 200 torr hydrogen; balance argon; total pressure 776 torr)

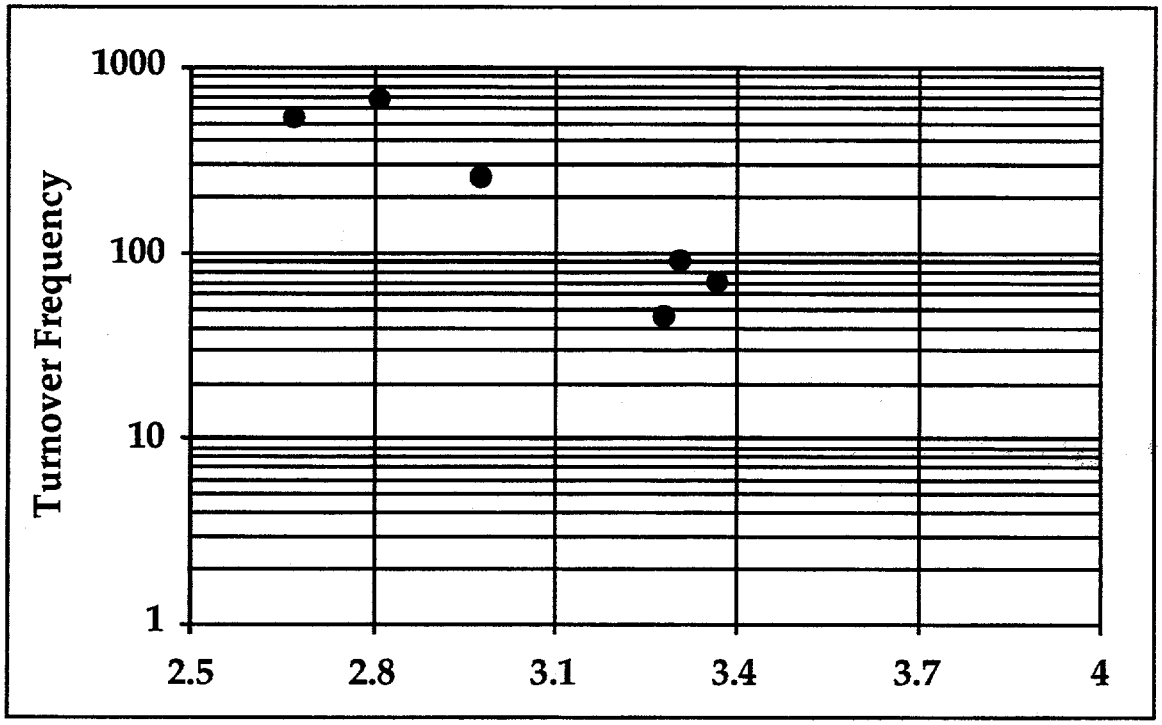

Figure 4.4. **Arrhenius plot for ethylene hydrogenation on Rh(755)**
(75 torr ethylene; 701 torr hydrogen; total pressure 776 torr)

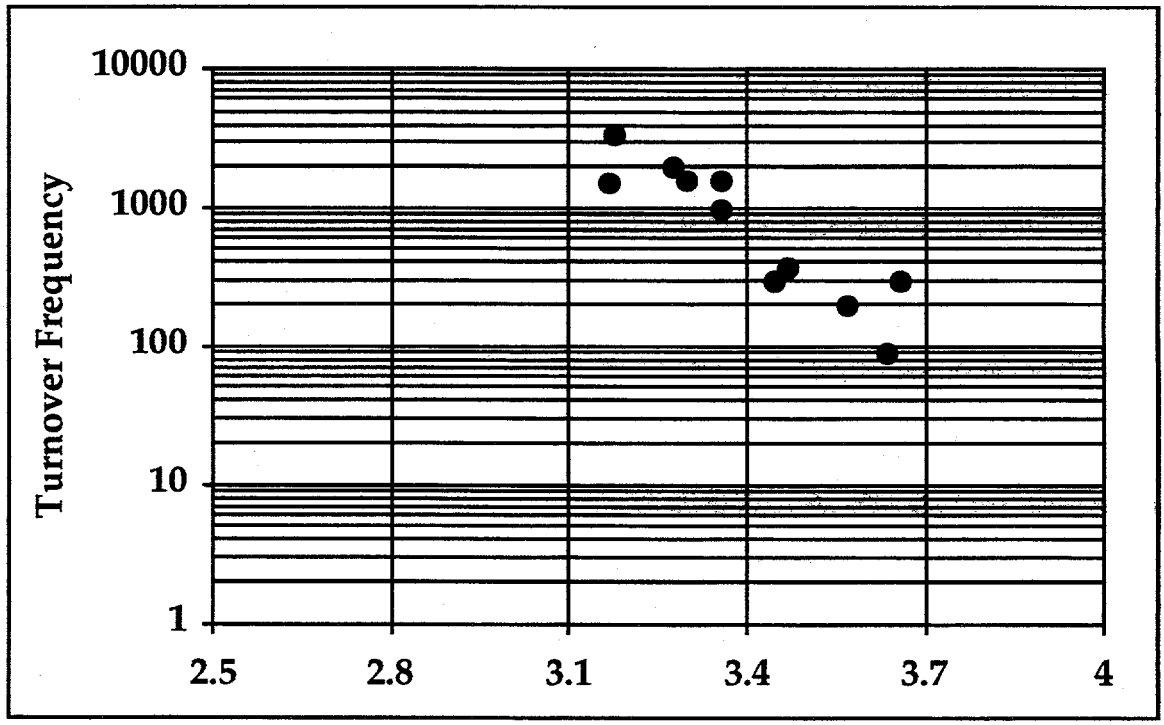

Figure 4.5. **Arrhenius plot for ethylene hydrogenation on Rh foil.**
(77 torr ethylene; 723 torr hydrogen; total pressure 800 torr)

4.2.2. Pt(111) and Pt foil

A Pt(111) sample was prepared as previously described. The specimen was elliptical in shape and exposed a total surface area of 1.56 cm^2 on its faces. The surface was tested for activity over the temperature range of 300-400 K at a total pressure of 800 torr using a reactive gas mixture consisting of a premixed cylinder of 10% ethylene in hydrogen. The results are presented in an Arrhenius plot form in Figure 4.6.

A 3 mil (0.008 cm) thick platinum foil sample was cut in a rectangular shape (1.0 X 0.7 cm) and cleaned in the same manner as the single crystal samples. The surface was tested for activity over the temperature range of 300-400 K at a total pressure of 800 torr using a reactive gas mixture consisting of a premixed cylinder of 10% ethylene in hydrogen. The results are presented in an Arrhenius plot form in Figure 4.7.

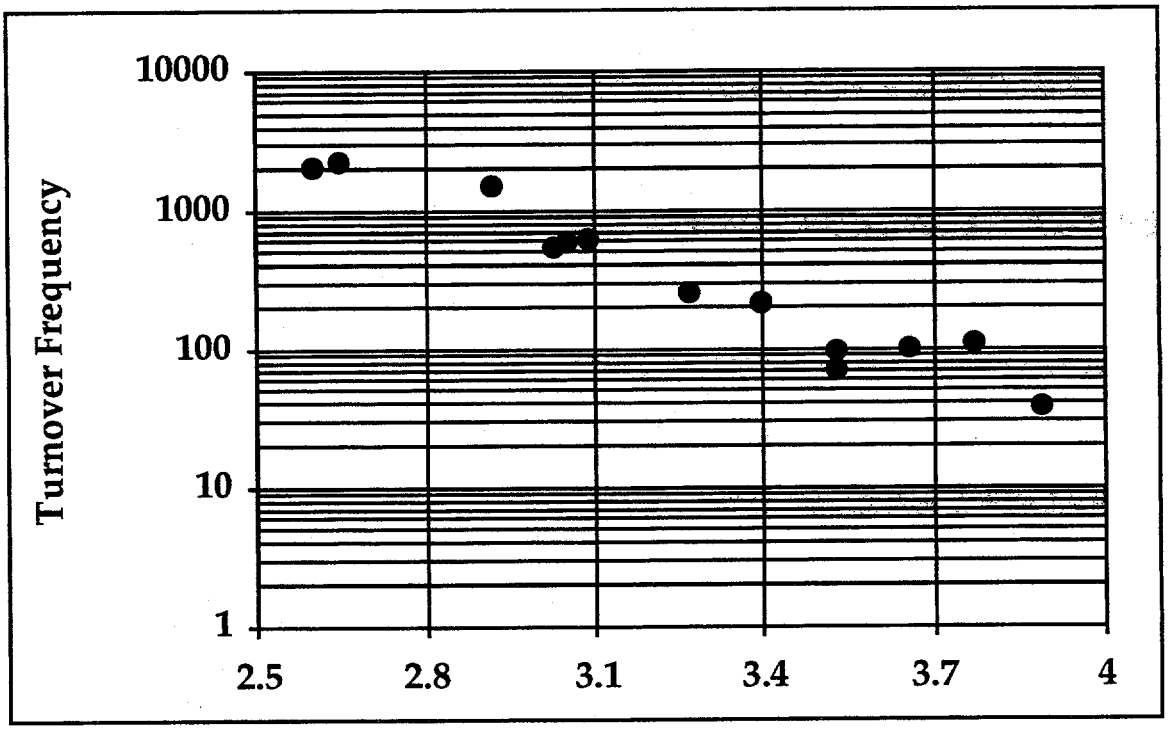

Figure 4.6. **Arrhenius plot for ethylene hydrogenation on Pt(111).**
(77 torr ethylene; 723 torr hydrogen; total pressure 800 torr)

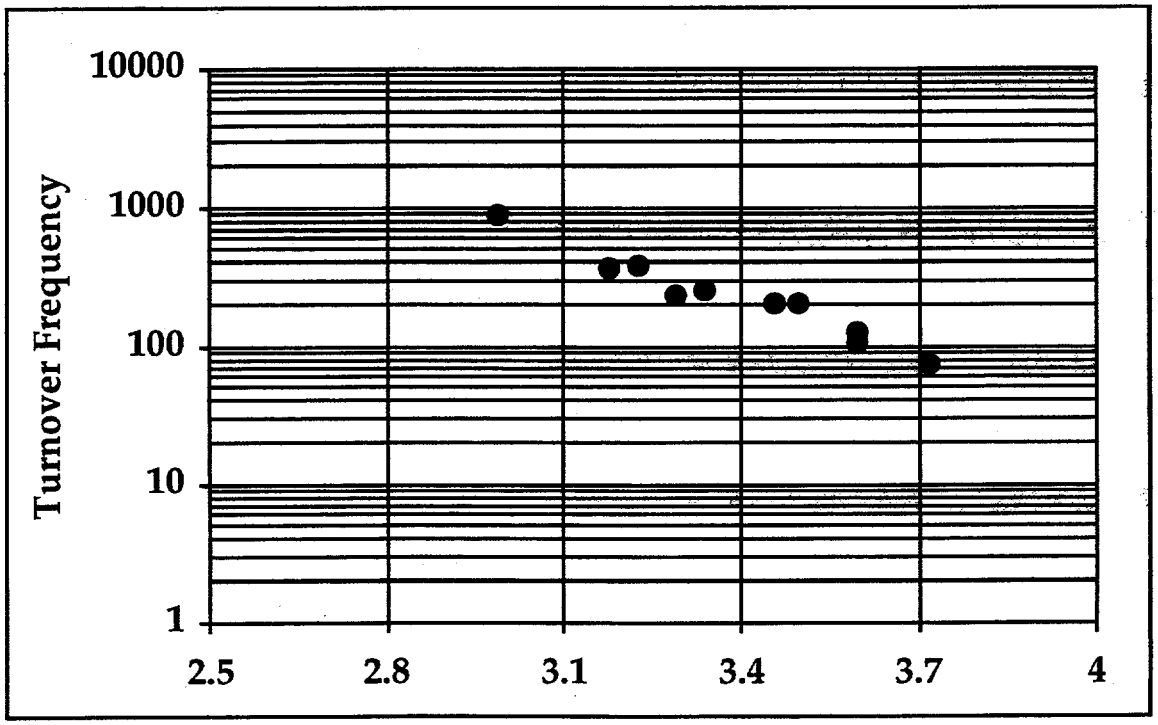

Figure 4.7. **Arrhenius plot for ethylene hydrogenation on Pt foil.**
(77 torr ethylene; 723 torr hydrogen; total pressure 800 torr)

4.23. Summary of kinetic results

Strictly speaking, it is not a valid procedure to compare the relative catalytic activity for two or more catalysts by simply stating the observed reaction rate at a given temperature. Even for identical reaction conditions, once you get away from a narrow temperature interval about the stated temperature, the relative reactivity may change due to differences in the activation energy. Assumptions made concerning the reaction orders in reactant partial pressures, may mask significant differences in activity even for comparisons made under isothermal conditions. Given all these caveats, the following comparisons of catalytic activity for the catalysts considered here is given for convenience.

Table 4.5. Ethylene hydrogenation activity for single crystal surfaces and foils.

Catalyst	TOF @ 300 K (s-1)	Activation Energy (kcal mol^{-1})	Temperature range (K)
Rh(755)	9×10^1	8 ± 2	300-375
Rh(111) [4]	5×10^1	7.5 ± 2	330-360
Rh foil	1.5×10^3	17 ± 4	270-315
Pt(111)	3×10^2	11 ± 2	245-385
Pt(111) [3]	7×10^1	10.9 ± 0.4	300-375
Pt foil	3×10^2	8 ± 2	270-335

Turnover frequencies (TOF) have been normalized to the following reaction conditions: 77 torr ethylene; 723 torr hydrogen; total pressure 800 torr, by using the assumption that the rate is first order in hydrogen partial pressure and zero order in olefin partial pressure. Rate measurements made at temperature ranges outside of 300 K have been graphically extrapolated from published figures to 300 K.

4. 3. High Temperature Kinetics

Previous investigations of the catalytic activity of both Pt and Rh surfaces were limited to temperatures < 370 K. In order to determine the possible role of the ethylidyne species on the catalytic activity, a series of higher temperatures experiments were planned which would attempt to measure the changes in activity across a range of reaction temperatures which span the decomposition temperature of the ethylidyne species. It should be recalled that the decomposition temperature of the ethylidyne species had previously been determined from temperature programmed desorption and vibrational studies (Table 4.6).

Using foil samples of each metal, reaction rates were measured at temperatures up to 500 K (Figures 4.8 and 4.9). However, for all temperatures in excess of 345 K for Pt and 315 K for Rh no further increase in the reaction rate was observed. For both metals, the maximum reaction rate reached 2000-3000 s^{-1}, indicating the onset of mass transfer control in the observed activity. The ability of the catalyst to no longer dependent on the rate of the surface reactions but now only depends on the rate of reactant diffusion to the surface or product diffusion away from the surface through the thin diffusion layer next to the surface. The Arrhenius plot shows a break from linearity because the rate is no longer exponentially dependent on temperature as for an activated process but rather has the approximately one half order dependence appropriate for a diffusion process. For the case of catalytic activity testing by supported catalyst, the transition from kinetic to mass

transfer control occurs is usually observed to occur more gradually because of the distribution in pore sizes inherent in such catalysts. The sharp break in the Arrhenius plot shown here is the result of the flat plate geometry of the catalyst with the array of uniform catalytic sites having equal access to the reactant film. This was the first recorded observation of reaction deliberately run in the mass transfer control regime in the Somorjai group. Attempts to extend the extend the temperature range by increasing the gas flow over the catalyst thereby decreasing the diffusion boundary layer thickness by increasing the recirculation pump speed were ineffectual due to the limited range of pumping speeds afforded by the pump. The effect of total pressure on the overall rate showed the expected first order dependence for a diffusion controlled reaction (Figure 4.10).

Table 4.6. **Ethylidyne decomposition temperatures on various platinum and rhodium surfaces.**

Ethylidyne Decomposition Temperatures

	(111)	(100)
Platinum	450 K [1]	not obs. [2]
Rhodium	400 K [3]	380 K [3]

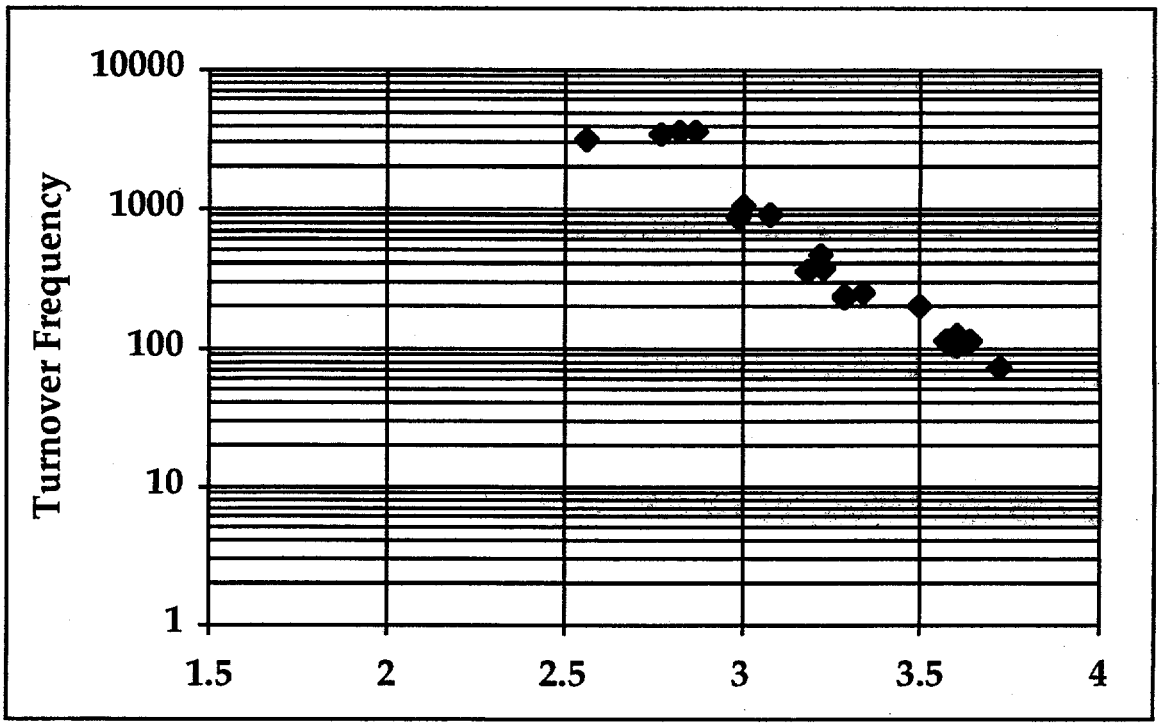

Figure 4.8. **Arrhenius plot for ethylene hydrogenation on Pt foil demonstrating the onset of mass transfer control at high temperatures (T>345 K).**
(77 torr ethylene; 723 torr hydrogen; total pressure 800 torr)

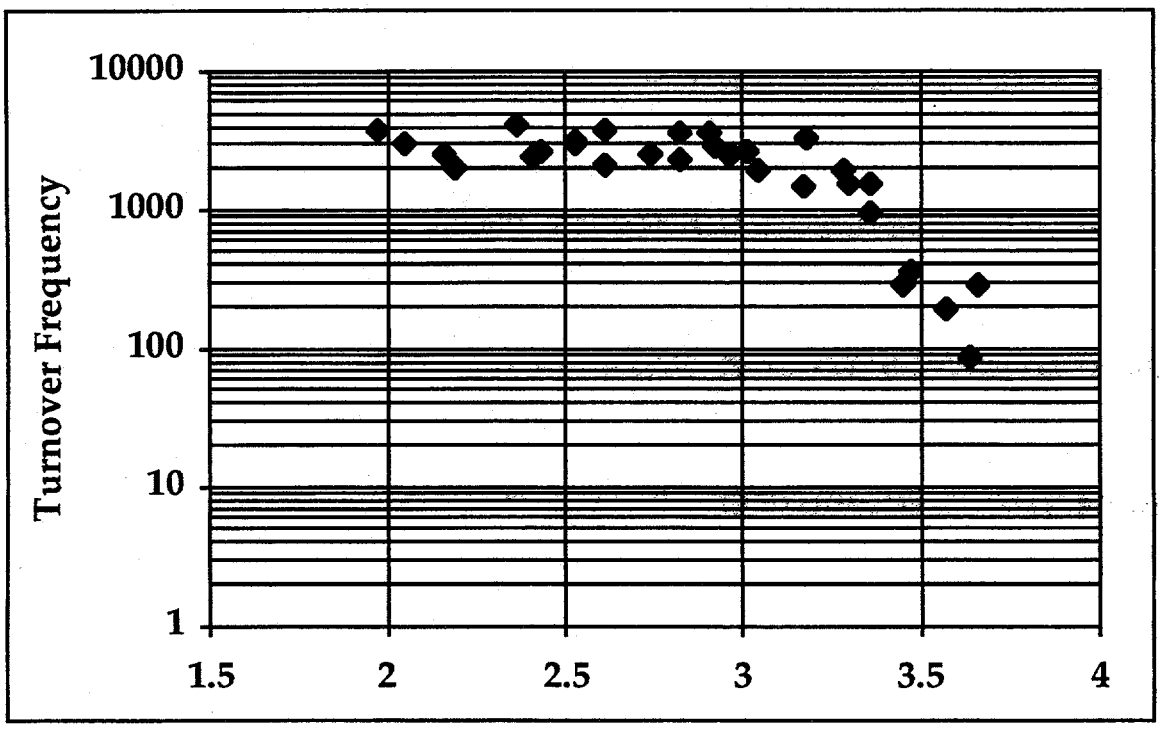

Figure 4.9. **Arrhenius plot for ethylene hydrogenation on Rh foil demonstrating the onset of mass transfer control at high temperatures (T> 315 K).**
(77 torr ethylene; 723 torr hydrogen; total pressure 800 torr)

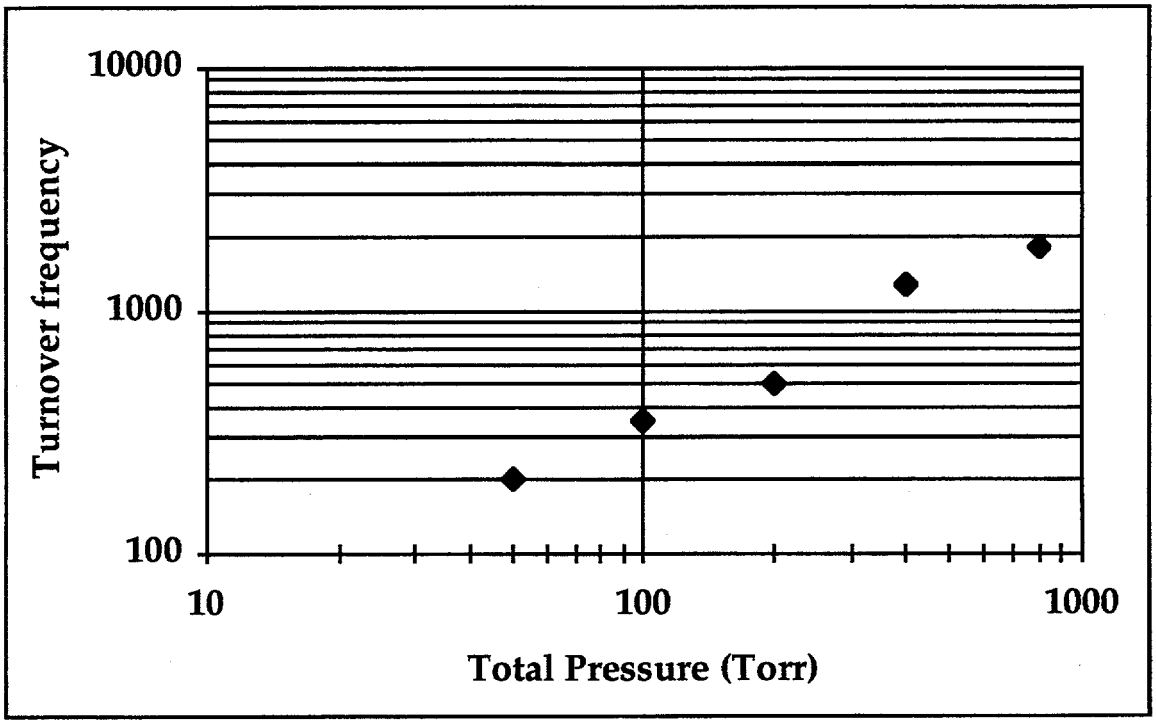

Figure 4.10. Effect of total reactant gas pressure on the rate of ethylene hydrogenation on Pt foil at high temperatures.
(9.66 v% ethylene in hydrogen; 385 K)

4.3.1. References

1. H. Steininger, H. Ibach and S. Lehwald, Surf. Sci. 117 (1982) 341.

2. E. Yagasaki, A. L. Backman, B. Chen and R. I. Masel, J. Vac. Sci. Technol. A8 (1990) 2616.

3. F. Zaera, Ph.D. thesis, University of California, Berkeley, 1984.

4. B. E. Bent, Ph.D. thesis, University of California, Berkeley, 1986.

5. Conclusions

5.1. Determination of the Degree of Structure Sensitivity

A comparison of the reactivity of Rh(111) [1] with Rh(755) allows a direct determination of the effect of step structure on ethylene hydrogenation activity. Structure sensitivity is expected to exhibit orders of magnitude differences in rate as particle size or surface orientation is varied. In this case, no significant differences were found confirming the structure insensitivity of this reaction over this metal. When the reported activity of the Rh(111) surface is normalized with respect to the partial pressures or reactants assuming a first order dependence in hydrogen and zero order in olefin, the activity of the Rh(755) surface determined in this work is in relatively good agreement. After correcting for the reaction conditions employed here, 77 torr ethylene with 723 torr hydrogen, at 300 K a turnover frequency of 9×10^1 s^{-1} is measured for the rhodium (755) surface compared to a turnover frequency of 5×10^1 s^{-1} for the Rh(111) surface. No real difference is rates may exist if the partial pressure dependence in hydrogen is actually slightly greater than one .

Rate measurements made on the Pt(111) surface and the Pt foil are in excellent agreement [Table 4.5]. No structure sensitivity is evident. Because a greater number of ethylene hydrogenation studies have used platinum catalysts, the results obtained in this work can be compared to others performed using different platinum catalysts (Figure 5.1).

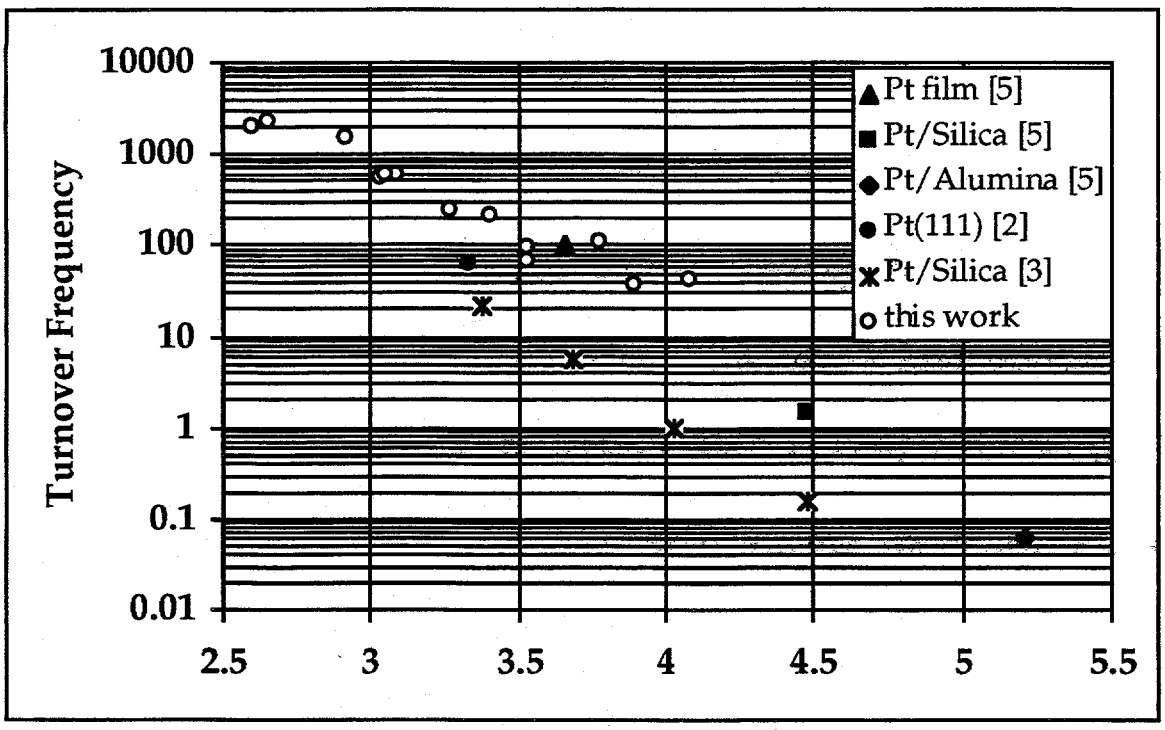

Figure 5.1. Ethylene hydrogenation activity for various platinum catalysts

(All results normalized to 77 torr ethylene; 723 torr hydrogen; total pressure 800 torr)

When these results are compared with those of a previous review, it can be seen that the rates obtained from the Pt(111) surface and the Pt foil (not shown for clarity, see Fig. 4.6) are in line with the earlier work. The previously cited anomalously low Pt(111) [2] result as well as the results of Dumesic [3] are shown for comparison.

5.2. The Relative Activity of Rhodium and Platinum

As for a comparison of the two metals, rhodium and platinum, the results are mixed. Rhodium foil is approximately five times more active than platinum foil at room temperature. For the reaction conditions chosen for comparison, 77 torr ethylene with 723 torr hydrogen at 300 K, a turnover frequency of 1.5×10^3 s^{-1} is measured for the rhodium foil compared to a turnover frequency of 3×10^2 s^{-1} for the platinum foil. This confirms the assignment of relative rates made in 1984 [2]. The opposite conclusion would be drawn when comparing the single crystal surface results. Here the rhodium catalyst is less active than the platinum, $5\text{-}9 \times 10^1$ s^{-1} vs. 3×10^2 s^{-1}, respectively. However, the measurements of the absolute activity of both of the rhodium single crystal surface may be in error. Most troubling is the fact that both of these rates are an order of magnitude less than that of the rhodium foil, 1.5×10^3 s^{-1}. Given that the foil surface is expected to comprise mainly of (111) and (100) planes with a large number surface defects, this discrepancy is surprising.

A reasonable explanation for the discrepancies in rates may involve the problem of boron contamination in the single crystal substrates not

observed in the foils. Boron contamination was discussed at length in Section 3.4. The persistence of boron on the surface, coupled with a virtual infinite reservoir in the bulk of the sample may be the root cause of these anomalously low rates. An excellent discussion of the role of surface impurities in obfuscating structure sensitivity studies can be found in the thesis of Sajkowki [4] for the case of ethylene oxidation over silver.
The good agreement between the single crystal sample of platinum and the platinum foil seems to argue against explanations which involve the physical form of the catalytic material, e. g. , that temperature measurements or temperature control is less precise on the foil vs. single crystal or that unaccounted for edge effects are dominating the behavior of the single crystal sample. For these reasons involving the probable role of boron contamination, the foil results are deemed more reliable.

5.3. The Role of Adsorbed Ethylidyne during Reaction

Under the reaction conditions employed in this work, it was impossible to measure the effect of running the ethylene oxidation reaction at temperatures greater than the decomposition temperature of the ethylidyne species. The onset of mass transfer control occurred at prior to reaching the temperature range of interest making direct comparison of rates in the presence and absence of the ordered overlayer of the ethylidyne species impossible.

5.3.1 References

1. B. E. Bent, Ph.D. thesis, University of California, Berkeley, 1986.
2. F. Zaera, Ph.D. thesis, University of California, Berkeley, 1984.
3. J. A. Dumesic et al, The Microkinetics of Heterogeneous Catalysis, American Chemical Society, Washington D. C., 1993.
4. D. J. Sajkowski, Ph. D. thesis, Stanford University, 1986.
5. F. J. Rivera-Latas, R. A. Dalla Betta and M. Boudart, AIChE. J. 38 (1992) 771.